Neurobiology of Disease 180 (2023) 106079

Contents lists available at ScienceDirect

Neurobiology of Disease

journal homepage: www.elsevier.com/locate/ynbdi

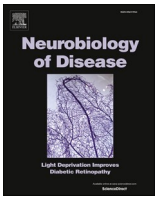

Rescue of synaptic and cognitive functions in polysialic acid-deficient mice and dementia models by short polysialic acid fragments

Hristo Varbanov [a,k,1], Shaobo Jia [a,1], Gaga Kochlamazashvili [b,c], Subhrajit Bhattacharya [d], Manal Ali Buabeid [e], Mohamed El Tabbal [a], Hussam Hayani [a], Stoyan Stoyanov [a], Weilun Sun [a], Hauke Thiesler [f], Iris Röckle [f], Herbert Hildebrandt [f,g], Oleg Senkov [a], Vishnu Suppiramaniam [e,h], Rita Gerardy-Schahn [f], Alexander Dityatev [a,b,i,j,*]

[a] German Center for Neurodegenerative Diseases (DZNE), Leipziger Str. 44, 39120 Magdeburg, Germany
[b] Department of Neuroscience and Brain Technologies, Istituto Italiano di Tecnologia, 16163 Genova, Italy
[c] Leibniz-Forschungsinstitut für Molekulare Pharmakologie (FMP), Robert-Roessle-Straße 10, 13125 Berlin, Germany
[d] School of Pharmaceutical and Health Sciences, Keck Graduate Institute, Claremont Colleges, Claremont, CA 91711, USA
[e] Department of Drug Discovery and Development, School of Pharmacy, Auburn University, Auburn, AL 36849, USA
[f] Institute for Clinical Biochemistry, Hannover Medical School, Carl-Neuberg-Str. 1, 30625 Hannover, Germany
[g] Center for Systems Neuroscience Hannover (ZSN), Bünteweg 2, 30559 Hannover, Germany
[h] College of Science and Mathematics, Kennesaw State University, GA 30144, USA
[i] Medical Faculty, Otto-von-Guericke-University, Magdeburg, Leipziger Str. 44, 39120 Magdeburg, Germany
[j] Center for Behavioral Brain Sciences (CBBS), Otto von Guericke University Magdeburg, Universitätsplatz 2, 39106 Magdeburg, Germany
[k] Institute of Neurophysiology, Hannover Medical School, OE 4230, Carl-Neuberg-Str. 1, 30625 Hannover, Germany

ARTICLE INFO

Keywords:
NCAM
NMDA receptor
Polysialic acid
Prefrontal cortex
Synaptic plasticity

ABSTRACT

Dysregulated cortical expression of the neural cell adhesion molecule (NCAM) and deficits of its associated polysialic acid (polySia) have been found in Alzheimer's disease and schizophrenia. However, the functional role of polySia in cortical synaptic plasticity remains poorly understood. Here, we show that acute enzymatic removal of polySia in medial prefrontal cortex (mPFC) slices leads to increased transmission mediated by the GluN1/GluN2B subtype of *N*-methyl-D-aspartate receptors (NMDARs), increased NMDAR-mediated extrasynaptic tonic currents, and impaired long-term potentiation (LTP). The latter could be fully rescued by pharmacological suppression of GluN1/GluN2B receptors, or by application of short soluble polySia fragments that inhibited opening of GluN1/GluN2B channels. These treatments and augmentation of synaptic NMDARs with the glycine transporter type 1 (GlyT1) inhibitor sarcosine also restored LTP in mice deficient in polysialyltransferase ST8SIA4. Furthermore, the impaired performance of polySia-deficient mice and two models of Alzheimer's disease in the mPFC-dependent cognitive tasks could be rescued by intranasal administration of polySia fragments. Our data demonstrate the essential role of polySia-NCAM in the balancing of signaling through synaptic/extrasynaptic NMDARs in mPFC and highlight the therapeutic potential of short polySia fragments to restrain GluN1/GluN2B-mediated signaling.

1. Introduction

The neural cell adhesion molecule (NCAM) is a transmembrane glycoprotein that promotes cell-cell and cell-extracellular matrix adhesion. During development, NCAM regulates multiple processes, such as neurite outgrowth, neuronal migration, and synaptogenesis (Duncan et al., 2021; Schnaar et al., 2014). In mammals, the functions of NCAM are changed dramatically by the two complementary polysialyltransferases ST8SIA2 and ST8SIA4, which add polysialic acid (polySia) to the extracellular domain of NCAM. PolySia is a linear homopolymer that is composed of varying numbers of sialic acid residues (Hildebrandt et al., 2010; Schnaar et al., 2014; Thiesler et al., 2022). In the mature hippocampus, polySia-NCAM is involved in *N*-methyl-D-aspartate receptor (NMDAR)-dependent synaptic plasticity (Becker

* Corresponding author at: German Center for Neurodegenerative Diseases (DZNE), Leipziger Str. 44, Haus 64, 39120 Magdeburg, Germany.
E-mail address: Alexander.Dityatev@dzne.de (A. Dityatev).
[1] Contributed equally to the study.

https://doi.org/10.1016/j.nbd.2023.106079
Received 22 January 2023; Received in revised form 4 March 2023; Accepted 8 March 2023
Available online 12 March 2023

et al., 1996; Bukalo and Dityatev, 2012; Kröcher et al., 2015; Luthi et al., 1994; Muller et al., 1996; Senkov et al., 2012; Varbanov and Dityatev, 2017). Mice deficient in NCAM show decreased levels of hippocampal long-term potentiation (LTP) and long-term depression in the hippocampus, accompanied by impaired spatial learning and fear conditioning (Cremer et al., 1994; Muller et al., 1996; Senkov et al., 2006; Stoenica et al., 2006). Similar deficits have been observed following acute polySia removal using endosialidases such as endoNF (Stummeyer et al., 2005) and/or genetic ablation of the polysialyltransferase ST8SIA4 (Becker et al., 1996; Eckhardt et al., 2000; Kröcher et al., 2015; Muller et al., 1996). In a previous study, we reported that polySia supports synaptic plasticity at hippocampal CA3-CA1 synapses and CA1-dependent contextual fear conditioning by restraining signaling through GluN2B-containing NMDARs (Kochlamazashvili et al., 2010). Mechanistically, polySia inhibits the activation of heterodimeric GluN1/GluN2B and heterotrimeric GluN1/GluN2A/GluN2B NMDARs by low micromolar concentrations of glutamate (Hammond et al., 2006a; Kochlamazashvili et al., 2010) that are characteristic for the extrasynaptic space.

Dysregulation of polySia predominantly carried by NCAM has been associated with several neuropsychiatric and neurodegenerative disorders, including schizophrenia, bipolar disorder, depression, and Alzheimer's disease (AD) (Brennaman and Maness, 2010; Sato and Kitajima, 2021; Thiesler et al., 2022). In AD patients, polySia-NCAM expression in the entorhinal cortex is significantly decreased and negatively correlated with hyperphosphorylated tau levels (Murray et al., 2016; Murray et al., 2018). In schizophrenia patients, post-mortem studies have shown reduced polySia-NCAM expression in the hippocampus and the dorsolateral PFC (Barbeau et al., 1995; Gilabert-Juan et al., 2012; Williams et al., 2020). In contrast, soluble fragments of the NCAM extracellular domain (NCAM-EC) are increased in the cerebrospinal fluid of patients with AD and schizophrenia (Honer et al., 1997; Strekalova et al., 2006; Todaro et al., 2004; Vawter, 2000; Vawter et al., 1998). Furthermore, a recent study demonstrated elevated serum levels of polySia-NCAM in schizophrenia, which might reflect enhanced proteolytic cleavage or clearance of polySia-NCAM from the brain. Notably, the increased polySia-NCAM serum levels correlate with negative and cognitive symptoms, and with decreased volume of Brodmann area 46 in the left PFC of schizophrenic patients. In support of the link between schizophrenia and polySia-NCAM, a recent microarray study has shown that the expression of the polysialyltransferase *ST8SIA4* gene is strongly downregulated in lymphoblastoid cell lines from antipsychotic-naïve first-episode schizophrenia patients (Gasso et al., 2017; Sato and Kitajima, 2021). However, there have been no causal studies investigating how the reduced polySia expression in the mPFC may affect cortical synaptic plasticity and cognitive functions.

Here, we demonstrate the impact of polySia on synaptic plasticity in the mPFC and in mPFC-dependent cognition using well-established models of polySia deficiency, namely, endosialidase treatment and polysialyltransferase-deficient mice. We found that deficiency in polySia results in an imbalance in signaling through synaptic/extrasynaptic NMDARs in the mPFC. Intranasal administration of short-chain polySia, as well as the rebalancing of synaptic/extrasynaptic NMDAR signaling by application of either GlyT1 or GluN1/GluN2B-NMDARs antagonists abrogated the effects of deficiency in polySia.

2. Materials and methods

2.1. Experimental design

The main aims of the present study were to investigate 1) how a deficit in polySia-NCAM leads to impaired PFC-dependent synaptic and cognitive functions, and 2) if small defined-size fragments of polySia, *e.g.* NANA12, consisting of 12 sialic acid (*N*-acetylneuraminic acid) residues in α2,8-linkage, are sufficient to rescue these functions by restoring the balance between synaptic and extrasynaptic NMDA receptors. To the first aim, we sought to determine the impact of acute enzymatic and chronic genetic ablation of polySia on synaptic and extrasynaptic glutamate NMDARs using whole-cell patch-clamp recordings in brain slices and HEK293 cells as a heterologous expression system. Further, we aimed to investigate the effects of polySia removal on synaptic plasticity in the mPFC using extracellular field potential recordings of LTP in brain slices in several rodent models of polySia dysregulation, including *ex vivo* and *in vivo* endoNF treatment and the mouse lines *St8sia4*$^{-/-}$ and *St8sia2*$^{-/-}$. To investigate the effects of polySia removal on PFC- and hippocampus-dependent learning, we used the novel object recognition task and the recency task. For the second aim, we tested whether these synaptic and behavioral deficits in polySia-deficient mice or in mice overexpressing mutated human microtubule associated protein Tau can be restored by *ex vivo* or *in vivo* intranasal application of short polySia fragments and the clinically used glycine transporter type 1 inhibitors sarcosine and SSR 504734. CNS delivery of NANA12 after intranasal administration was confirmed using two-photon imaging of fluorescently-tagged NANA12 in the PFC of anesthetized polySia-deficient mice.

In all behavioral tests, the researcher was blind to mouse genotype and treatment, and the objects were randomly assigned and counterbalanced within a trial. The phenotypes of *St8sia4*$^{-/-}$ and *St8sia4*$^{+/+}$ mice in the novel object recognition test were reproduced by a second researcher using a different cohort of mice. Impairment of LTP in *St8sia4*$^{-/-}$ mice was reproduced by a second researcher under similar experimental conditions. Sample sizes in electrophysiological and behavioral experiments followed previous publications using the same methods (Brennaman et al., 2011).

For patch-clamp recordings of EPSCs in neurons, cells in which R_s changed by >20% throughout the experiment were excluded from the data analysis (1 in Fig. 1D; 4 in Fig. 1H; 3 in Fig. 3B; 2 in Fig. 5B, C; 1 in Fig. S8A). For fEPSP recordings in brain slices, the slices in which the fiber volley amplitude of the fEPSP changed by >15% were excluded from the data analysis (8 in Fig. 4A; 4 in Fig. 4I; 3 in Fig. 5D; 3 in Fig. S8C).

To ensure proper evaluation of memory function in the NORT and recency test, anxious mice that may stay in the corners of the test arena instead of exploring it and objects need to be excluded. Here, out of 102 mice we excluded 7 mice whose cumulative exploration time to both objects were <10 s in a 10-min test session (1 in Fig. 6C; 1 in Fig. 6D; 1 in Fig. 7D, 1 in Fig. 7E (left); 1 in Fig. 7E (right)). The effective sample sizes for each graph are specified in the respective paragraphs and figure legends.

2.2. Animals

All treatments and behavioral procedures were conducted in accordance with animal research ethics standards defined by German law and approved by the Ethical Committee on Animal Health and Care of the State of Saxony-Anhalt (42502–2-1159 DZNE, 42502–2-1343 DZNE, and 42,502–2-1346 DZNE) or by the Italian Committee on Animal Health and Care of the governmental body in Rome.

C57BL/6J mice were bred at the animal facility of DZNE Magdeburg. Constitutively ST8SIA4-deficient mice (*St8sia4*$^{-/-}$) (Eckhardt et al., 2000) were backcrossed with C57BL/6 J mice for >8 generations. Mice heterozygous for *St8sia4* were crossed to produce homozygous mutants and littermate wild-type controls. As a model of amyloidosis, 5xFAD mice (B6.Cg-Tg(APPSwFlLon,PSEN1*M146L*L286V)6799Vas/Mmjax from the Jackson Laboratory) inbred on C57BL6J background for >5 generations were used. These mice overexpress both mutant human amyloid beta (A4) precursor protein 695 (APP) with the Swedish (K670N, M671L), Florida (I716V), and London (V717I) Familial Alzheimer's Disease (FAD) mutations and human PS1 harboring two FAD mutations, M146L and L286V. Expression of both transgenes is regulated by neural-specific elements of the mouse *Thy1* promoter to drive overexpression in the brain. This line was maintained at the animal

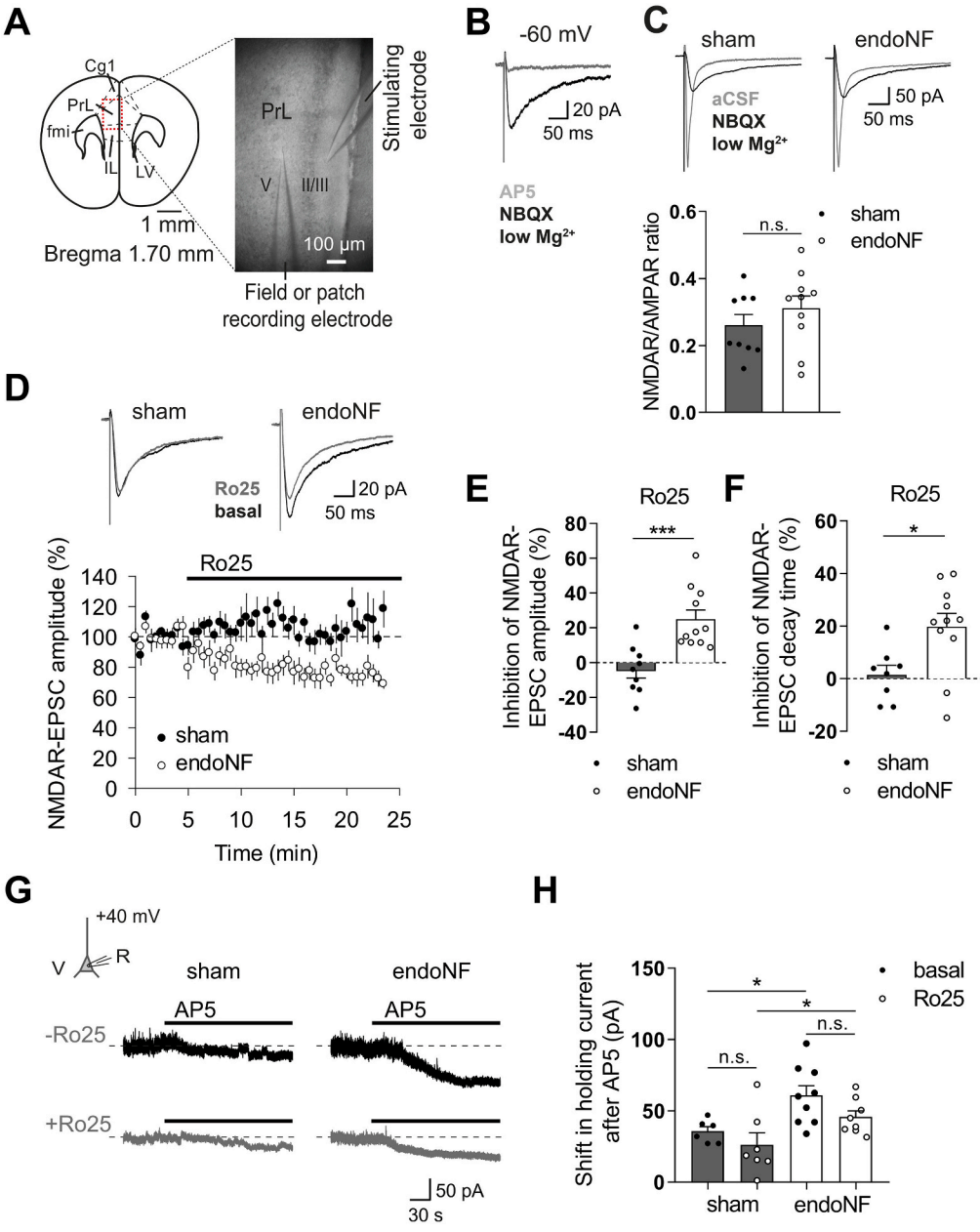

Fig. 1. Effects of endoNF treatment on evoked and tonic NMDAR-mediated currents in mPFC slices.

(A) A representative coronal section through the mPFC (left) and a photomicrograph (4× objective) illustrating locations of electrodes for recordings of evoked EPSCs or fEPSPs (right). Cg1, cingulate; PrL, prelimbic; IL, infralimbic cortex; II/III, V, cortical layer; fmi, forceps minor of the corpus callosum; LV, lateral ventricle.

(B) Representative examples of averaged evoked NMDAR-EPSCs from layer V pyramidal neurons, which were pharmacologically isolated at −60 mV in modified aCSF containing low Mg^{2+} (0.1 mM), the selective antagonist of AMPA)/kainate receptors NBQX (10 µM), and the selective antagonist of $GABA_B$ receptors CGP-55845 (2 µM) (black). Bath application of the NMDAR-selective antagonist AP5 (50 µM) blocked these slow EPSCs almost completely (gray).

(C) Representative examples (top) of fast AMPAR-EPSCs at −60 mV in normal aCSF (gray) and slow NMDAR-EPSCs in the presence of low Mg^{2+} (0.1 mM), NBQX (10 µM), and CGP-55845 (2 µM) (black). A bar graph (bottom) showing similar NMDAR/AMPAR ratio in endoNF- and sham-treated slices (n/N: 9/10 and 10/8, respectively; $P = 0.313$, unpaired Student's *t*-test).

(D) Examples (top) and time courses of normalized amplitudes (bottom) of evoked NMDAR-EPSCs before (basal, black) and after bath application of GluN1/GluN2B antagonist Ro 25–6981 (Ro25, 0.3 µM, gray). The mean amplitude recorded during a 5-min baseline period before Ro 25–6981 application was taken as 100%.

(E, F) Increased Ro 25–6981 (0.3 µM)-mediated inhibition of amplitude (***$P < 0.001$, unpaired Student's *t*-test) and of decay time (*$P < 0.05$, unpaired Student's *t*-test) of NMDAR-EPSCs in endoNF-treated slices compared with sham controls (n/N: 9/9 in sham group, 1 outlier excluded for dacay time; 11/8 in endoNF group). Recordings in B–F were performed in voltage-clamp mode (holding potential −60 mV), and EPSC examples represent averages of 8–10 traces. Amplitude (E) and decay time (F) of evoked NMDAR-EPSCs were measured during 5 min before (basal) and during 10–15 min after application of Ro25.

(G) Representative traces of NMDAR-mediated holding currents (holding potential +40 mV) before and after bath application of AP5 (50 µM). The inset shows experimental design for tonic currents. Horizontal dotted lines indicate the basal level of holding current before AP5.

(H) Quantification of tonic NMDAR-mediated currents recorded in the presence or absence Ro 25–6981 (0.3 µM). Two-way ANOVA revealed significant difference between sham and endoNF treated groups ($P = 0.0018$). *$P < 0.05$, Holm-Sidak *post hoc* test. Numbers of mice used: 4 for Sham, Sham+Ro25, endoNF+Ro25, 6 for endoNF. Data are shown as mean ± SEM.

facility of DZNE Magdeburg. Heterozygous mice were crossed with C57BL/6J mice to produce heterozygous and wild-type littermate controls.

For electrophysiological experiments in brain slices, we used adult 2- to 4-month-old C57BL/6J (control and treated with endoNF) as well as *St8sia4*$^{-/-}$ mice and their respective age-matched wild-type littermates of both sexes. For behavioral experiments, we used 2- to 3-month-old C57BL/6J males (control and treated with endoNF) and 7- to 10-month-old *St8sia4*$^{-/-}$ males and their wild-type littermates. All mice were kept in a reverse light-dark cycle (12:12 h, light on at 9:00 pm) with food and water *ad libitum*, and they were tested during the dark phase of the cycle when mice are active.

2.3. Electrophysiological recordings

Coronal slices containing the mPFC were incubated in aCSF without (sham) or with the addition of endoNF (10 μg/ml) at 35 °C for 2 h. Field EPSP recordings were performed in 400-μm-thick mPFC slices, as described elsewhere (Brennaman et al., 2011).

Evoked NMDAR-mediated EPSCs from layer V pyramidal neurons in mPFC slices were recorded in voltage-clamp mode, at a holding potential of −60 mV, and pharmacologically isolated, as reported previously (Chen et al., 2003). Tonic NMDAR-mediated holding currents were recorded and pharmacologically isolated at +40 mV, as described elsewhere. Bursts of IPSCs were evoked by TBS at holding potential 0 mV in normal aCSF. Before TBS application, 10 EPSCs were evoked by single pulses at 0.033 Hz at −60 mV in normal aCSF in both sham- and endoNF-incubated slices. The stimulation intensity was set to produce EPSCs with the mean amplitude of approximately 100 pA in all slices. For electrophysiological recordings in brain slices, numbers of cells/slices recorded (n) and mice used (N) were presented as “n/N". All data are shown as the mean ± SEM.

For detailed descriptions of the brain slice preparation, whole-cell patch-clamp recordings in slices and transfected HEK293 cells, field EPSP recordings of LTP, reagents used, numbers of cells/slices recorded (n) and mice used (N), data analysis, and statistics for slice electrophysiology, please see Supplementary materials and methods.

2.4. Immunohistochemistry

To assess whether polySia was removed successfully by endoNF, sham- and endoNF-incubated coronal mPFC and hippocampal slices (400 μm) from *Thy1*-EGFP mice were fixed in 4% paraformaldehyde in phosphate buffer (PB, 0.24 M, pH 7.2) for 3 h at room temperature and cryoprotected with 30% sucrose in PB at 4 °C overnight. The tissue processing, immunostaining, and imaging were performed as described elsewhere (Eckhardt et al., 2000) with some modifications, as outlined in Supplementary materials and methods.

2.5. Novel object recognition test

A white open field arena (50 × 50 × 30 cm) was used in the novel object recognition task. All behavior was video recorded and analyzed automatically by software (ANY-maze, version 4.99, Stoelting Co., Wood Dale, IL). The test was performed using a standard protocol that includes two phases: a) a familiarization/encoding phase: mice were placed for 10 min in the arena, during which they have to explore two identical objects positioned in the center of the arena; b) a test/retrieval phase: one familiar object and one novel object were placed in the center of the arena, and mice were allowed to explore for 10 min. In the same trial, objects were counterbalanced, and between trials, different sets of objects were used. The interval between the encoding and retrieval phases was 2 h.

2.6. Recent object recognition test

The “recency” test comprised two encoding phases followed by a retrieval phase, modified from (Nelson et al., 2011). The interval between the encoding phases was 1 h, and the interval between the second encoding phase and the retrieval phase was 10 min. In the first encoding phase, animals were placed into the open field arena and allowed to explore a pair of identical objects for 10 min. Then, a different pair of identical objects was presented in the second encoding phase (10 min total exploration time). During the retrieval phase, two different objects, one object from each encoding phase, were placed into the apparatus and animals were given 10 min to explore them.

2.7. EndoNF injection in vivo

For acute intra-mPFC injection of endoNF (2 μg/μl per site) or vehicle as deep as 1.5 and 2.25 mm from the brain surface, stainless steel guide cannulas made in-house were stereotaxically implanted similarly as described for intrahippocampal injections with the following coordinates: AP +1.9 mm; ML ±0.5 mm from bregma and the midline, respectively, according to the mouse brain atlas. All behavioral experiments were performed after the mice had fully recovered (5–7 d after surgery) and regained their normal weight. More detailed protocols and description of the statistical analysis are provided in Supplementary materials and methods.

2.8. Drug administration in behavioral experiments

Mice underwent saline (0.9% NaCl) or sarcosine (600 mg/kg b.w., i.p., Sigma Aldrich, Germany) injection 30 min before the encoding phase in all tested groups (C57BL/6 J injected with endoNF in the mPFC, and *St8Sia4*$^{-/-}$ *versus* *St8Sia4*$^{+/+}$). NANA12 (NANA designates polySia fragments and numbers indicate the fragment size, *i.e.* NANA12 is an oligomer with 12 sialic acids in α2,8-linkage) or control NANA1 (free sialic acid) were delivered intranasally as 4 × 4-μl injections (1 mg/ml) in each nostril of the mouse (32 μl per mouse in total) 30 min before a cognitive test. DMB-labeled NANA2 (DMB-NANA2) and NANA12 (DMB-NANA12) were applied intranasally (2 mg/ml, as described above) 30 min before the cognitive tests were performed with *St8Sia4*$^{-/-}$ and *St8Sia4*$^{+/+}$ mice. The synthesis and purification of DMB-NANAs followed published protocols (Keys et al., 2012).

3. Results

3.1. Increased evoked GluN2B-mediated currents after enzymatic removal of polySia

To examine the functions of polySia in the mPFC, we treated acute mPFC slices with the polySia-degrading enzyme endoNF, which has been shown to digest polySia in hippocampal slices (Kochlamazashvili et al., 2010). To confirm that polySia is efficiently removed and to examine its expression in relationship to mPFC pyramidal neurons, we performed immunohistochemistry for polySia in sham- and endoNF-incubated hippocampal and mPFC slices from *thy1*-EGFP mice. These mice show expression of the enhanced green fluorescent protein (EGFP) under the control of the *Thy1* promoter in a subset of cortical layer V pyramidal neurons (Feng et al., 2000). In sham-treated slices, polySia was highly expressed in the hippocampal mossy fibers and in all layers of the mPFC (Fig. S1A left). In sham-treated mPFC slices, EGFP-expressing proximal dendrites of layer V pyramidal neurons were embedded in dense, diffusely polySia-labeled structures, which were present in close proximity to dendritic spines (Fig. S1B left). In endoNF-treated mPFC slices, polySia immunolabeling was practically absent (Fig. S1A middle; S1B right). As a positive control for endoNF enzymatic activity, we also verified that the characteristic polySia labeling of mossy fibers (Eckhardt et al., 2000) was lost in hippocampal slices treated with endoNF

(Fig. S1A middle), as shown previously (Kochlamazashvili et al., 2010).

To study the functional impact of polySia on excitatory transmission in the mPFC, we applied electrical stimulation to layer II/III and recorded evoked EPSCs from layer V pyramidal cells (Fig. 1A) in sham- and endoNF-treated slices from adult C57BL/6J mice. Following initial recording of mixed excitatory postsynaptic currents (EPSCs) in normal aCSF (mediated by AMPARs and NMDARs, gray trace in Fig. 1C), the NMDAR-mediated component (black traces in Fig. 1B, C) of EPSCs was pharmacologically isolated at a membrane holding potential of −60 mV, in modified aCSF containing low Mg^{2+} (0.1 mM), the selective antagonist of α-amino-3-hydroxy-5-methyl-4-isoxazolepropionic acid (AMPA)/kainate receptors NBQX (10 μM), and the selective antagonist of γ-aminobutyric acid $(GABA)_B$ receptors CGP-55845 (2 μM) as reported earlier (Chen et al., 2003). The isolated NMDAR-EPSCs could be almost completely blocked by application of the competitive NMDAR antagonist AP5 (Fig. 1B). The ratio between NMDAR- and AMPAR-mediated current amplitude in endoNF-treated slices was not different from that recorded in sham-treated slices (Fig. 1C). Since the mean amplitude of mixed AMPAR-mediated currents in normal aCSF (gray) was similar under both conditions (sham, 304.64 ± 11.87 pA; endoNF, 307.54 ± 13.79 pA, $P = 0.875$), the unaltered NMDAR / AMPAR ratio suggests that endoNF treatment did not change the total NMDAR-mediated current.

Because polySia inhibits GluN2B-containing NMDARs only at the low glutamate concentrations characteristic of the extrasynaptic space (Kochlamazashvili et al., 2010) and because most extrasynaptic NMDARs are thought to be GluN2B heterodimers, it is plausible that polySia specifically inhibits extrasynaptic NMDARs. To test whether the activity of GluN2B-containing extrasynaptic NMDARs is elevated after polySia removal, as reported for CA1 pyramidal cells (Kochlamazashvili et al., 2010), we recorded evoked NMDAR-EPSCs at room temperature before and after addition of the GluN2B-specific antagonist Ro 25–6981 (Fischer et al., 1997), at a low micromolar concentration (0.3 μM). We selected this antagonist concentration because 0.3–1 μM Ro 25–6981 produces maximal inhibition (~70%) of heterodimeric GluN1/GluN2B-NMDARs expressed in HEK293 cells (half-maximal inhibitory concentration $IC_{50} = 0.05$ μM), while GluN1/GluN2A-NMDARs are inhibited at >10 μM Ro 25–6981 ($IC_{50} > 65$ μM) (Volianskis et al., 2013). Moreover, previous data have demonstrated that at 22 °C, but not at 35 °C, a single stimulus can lead to glutamate spillover (Asztely et al., 1997) and hence to activation of extrasynaptic NMDARs. In endoNF-treated slices, but not in sham-treated mPFC slices, we revealed a significant inhibition of both amplitude (~25%, Fig. 1D, E; for absolute values, see Fig. S2, left) and decay time (~20%, Figs. 1F and S2, right) of evoked NMDAR-EPSCs after Ro 25–6981 application. Both of these results are consistent with an elevation of transmission through GluN1/GluN2B-NMDARs in polySia-deficient slices because these receptors have a slower decay time compared to GluN2A-containing receptors. As total NMDAR currents in the prefrontal cortex (which are the sum of currents mediated by GluN2A- and GluN2B-containing NMDARs) are not affected by endoNF (Fig. 1C), the observed increase in GluN2B-mediated transmission presumably occurs at the expense of transmission through GluN2A-containing NMDARs.

3.2. Increased tonic NMDAR-mediated currents after endoNF treatment

As another approach to verify the effect of polySia on extrasynaptic NMDARs, we analyzed tonic NMDAR currents in mPFC pyramidal cells, which are presumably mediated by the tonic activation of extrasynaptic NMDARs. To assess the level of activation of extrasynaptic NMDARs in the absence of polySia, we recorded NMDAR-mediated holding currents at a holding potential of +40 mV from layer V pyramidal neurons and measured the shift in holding current after application of the NMDAR-selective antagonist AP5. Since no synaptic stimulation was delivered, this shift provides a measure of the tonic activation of extrasynaptic NMDARs (Le Meur et al., 2007; Papouin et al., 2012). The shift in NMDAR-mediated tonic current was markedly increased in endoNF-incubated slices compared with sham-treated slices (Fig. 1G, H), indicating an overactivation of extrasynaptic NMDARs in the absence of polySia. When we repeated these experiments in the presence of Ro 25–6981 (0.3 μM), there was no significant difference in the shift in tonic current in endoNF- and sham-treated slices (Fig. 1G, H), which is consistent with an increased contribution of GluN1/GluN2B heterodimers in endoNF-treated slices. Interestingly, a substantial fraction of tonic currents in sham-treated slices was not affected by a low concentration of Ro 25–6981. This finding suggests that a large fraction of tonically-activated extrasynaptic NMDARs in the mPFC are GluN1/GluN2A/GluN2B heterotrimers rather than GluN1/2B heterodimers, as previously reported in the hippocampus and other areas of the brain (Bhattacharya et al., 2018; Hansen et al., 2014; Paoletti et al., 2013; Papouin and Oliet, 2014; Yi et al., 2019).

3.3. Inhibition of GluN2B-EPSCs in HEK293 cells and mPFC slices by polySia fragments

We have shown previously that a mixture of sialic acid polymers in the form of colominic acid or its subfraction with polymer chains ranging in size between 25 and 50 residues, but not free sialic acid, inhibits NMDAR-mediated currents activated by low micromolar concentrations of glutamate (Hammond et al., 2006a). As a next step towards the therapeutic use of polySia, we investigated whether short, defined-length fragments of polySia (12 sialic acid residues, NANA12) would modulate NMDARs. In HEK293 cells expressing GluN1/GluN2B receptors, NANA12 at 1 μg/ml (≈ 0.3 μM) strongly inhibited whole-cell currents activated by application of 3 μM glutamate (Fig. 2A), in line with previous recordings showing the effect of colominic acid on the open probability of GluN1/GluN2B channels (Hammond et al., 2006a). To verify that NANA12 acts on the open probability, current amplitude histograms were obtained from single GluN1/GluN2B channel recordings (Fig. 2B-C) in the presence of 3 μM glutamate alone (control), or in combination with 0.2, or 0.3, or 0.4 μg/ml NANA12. Comparison of single-channel conductance between groups showed no significant changes across treatments (Fig. 2D, right). However, the open probability of the GluN2B-NMDAR channels was significantly decreased in a concentration-dependent manner in the presence of different concentrations of NANA12 compared with the untreated control, indicating that the oligomer influenced this specific ion channel property of NMDAR subunits (Fig. 2D, left). To study if there was time-dependent desensitization of NMDARs during drug applications, the open probabilities of channels were measured at the beginning and the end of treatment with 3 μM glutamate alone and in combination with 0.2 μg/ml NANA12. No effect of time was revealed on the open probability of the GluN2B-NMDAR channels (Fig. S4). Hence, the effects observed were solely due to NANA12 rather than channel desensitization (for methods please refer to Supplementary Information) (Bhattacharya et al., 2018; Hammond et al., 2006b).

Next, we recorded evoked NMDAR-EPSCs in mPFC slices and tested whether NANA12 would occlude their inhibition by Ro 25–6981 (Fig. 3A, B). In sham-treated slices, we found no significant inhibition of NMDAR-EPSC amplitude by NANA12 or subsequently applied 0.3 μM Ro 25–6981. In contrast, in endoNF-treated slices, NANA12 inhibited significantly NMDAR-EPSC amplitude (~25% decrease) at the concentration of 1 μg/ml. Subsequent application of Ro 25–6981 reduced NMDAR-EPSC amplitude marginally (Fig. 3A, B). NANA12 reached ~90% of the mean inhibition caused by application of Ro 25–6981 to endoNF-treated slices (Figs. 1D and 3D). Thus, in slices depleted of polySia by endoNF treatment, ≈ 0.3 μM NANA12 and 0.3 μM Ro 25–6981 inhibit NMDAR-EPSCs to a similar extent.

To test whether the effects of the negatively charged NANA12 were specific, we repeated these experiments using monomers of sialic acid (NANA1), which are also negatively charged but do not inhibit NMDAR-mediated currents in cultured hippocampal neurons (Hammond et al.,

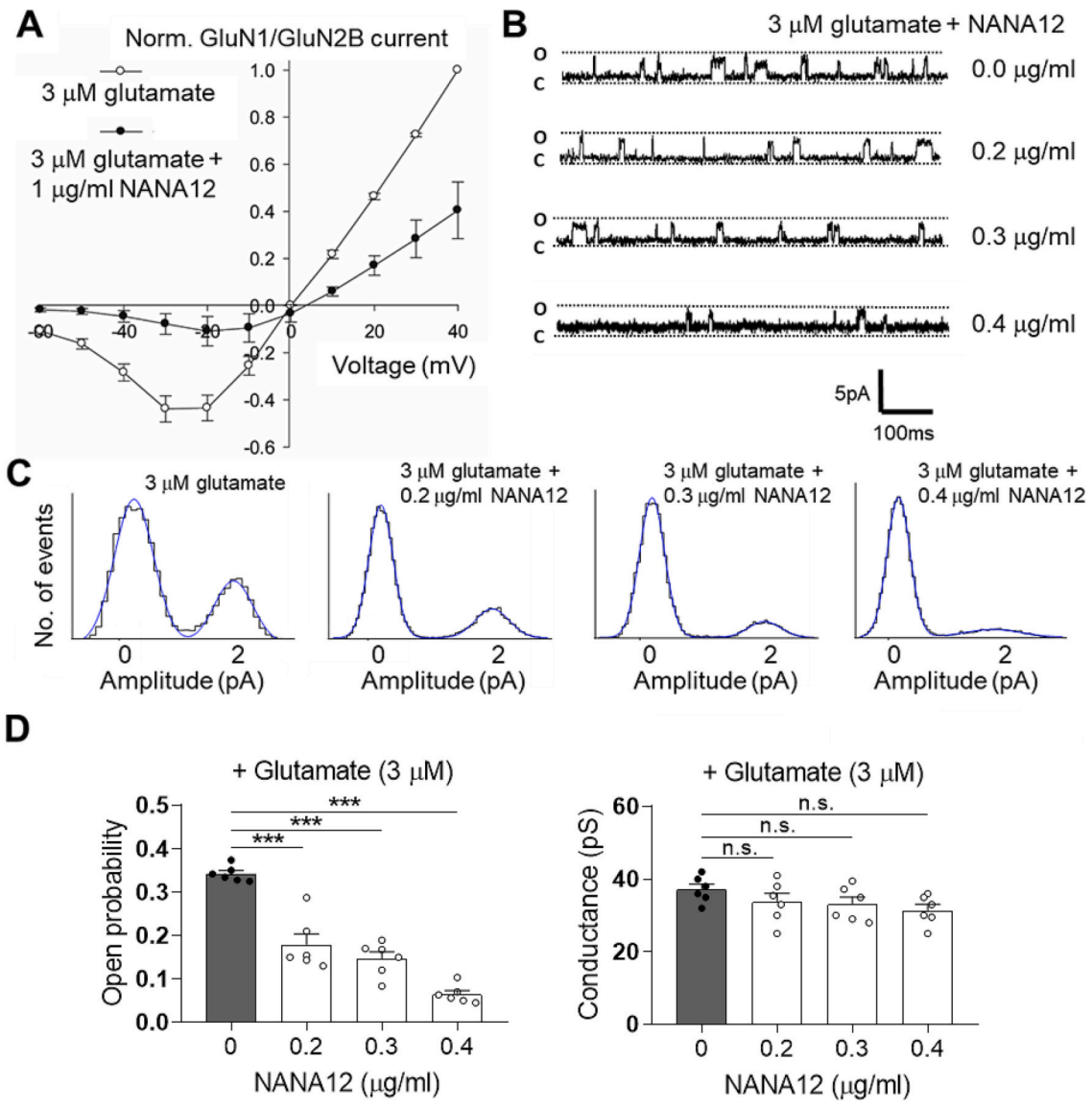

Fig. 2. Effects of NANA12 on glutamate-induced GluN1/GluN2B-mediated currents in HEK-293 cells and lipid bilayers.
(A) Analysis of whole-cell-patch-clamp-currents elicited by 3 μM glutamate in HEK293 cells co-transfected with EGFP, GluN1, and GluN2B. The currents were normalized using the value of current activated at +40 mV, in the absence of NANA12. Two-way repeated measures ANOVA revealed a significant effect of voltage and interaction between voltage and treatment (both $p < 0.001$).
(B) Representative GluN1/GluN2B single-channel recordings (voltage-clamped at +80 mV) in the presence of 3 μM glutamate alone (control), or in combination with 0.2, 0.3 or 0.4 μg/ml NANA12. C and O, closed and open states.
(C) Current amplitude histograms corresponding to (B) and their fit by a mixture of two Gaussians corresponding to the closed and open state, respectively.
(D) Comparison of single-channel open probability (left) and conductance (right) in the presence of different NANA12 concentrations compared with the control, one-way repeated measures ANOVA with a Dunnett's *post hoc* test, ***$P < 0.001$, $n = 6$. Data are shown as mean ± SEM.

2006a). NANA1 had no effect on the amplitude of NMDAR-EPSCs in endoNF-treated mPFC slices (Fig. 3C, D), whereas the subsequent application of 0.3 μM Ro 25–6981 significantly reduced (by ~20%) the EPSC amplitude (Fig. 3C).

Next, we tested the impact of shorter sialic acid oligomers such as NANA5. NANA5 (1 μg/ml and 10 μg/ml) reduced the amplitude of NMDAR-EPSCs in endoNF-treated slices, and this effect was significantly different from that of NANA1 (Fig. 3D). This suggests that five residues of sialic acid are sufficient to inhibit evoked NMDAR-EPSCs, although less efficient than fragments comprising 12 residues.

Another attractive option to compensate for polySia deficiency would be to use small polySia mimetics. One of these is tegaserod, a serotonin 5-HT_4 receptor agonist that is a clinically approved drug for the treatment of irritable bowel syndrome and constipation (Muller-Lissner et al., 2001). Molecular modeling and docking studies have shown that tegaserod might potentially compete with polySia for binding to the polySia binding site of antibody 735 (Bushman et al., 2014). The polySia-mimicking activity of tegaserod to stimulate peripheral nerve regeneration has been shown *in vitro* and *in vivo* and found to be independent of its described function as a 5-HT_4 receptor agonist (Bushman et al., 2014). Given the potential of polySia to regulate GluN2B-NMDARs, we examined whether tegaserod may exhibit similar inhibitory effects on NMDAR-EPSCs. Whole-cell recordings in the presence of a 5-HT_4 antagonist revealed strong inhibition of NMDAR-EPSC amplitude by tegaserod in both sham- (~50%) and endoNF-treated slices (~30%), which were not significantly different from each other (Fig. S5). This is in contrast to the predominant effects of GluN2B-inhibitor Ro25–6981 and NANA12 on endoNF-treated slices. These

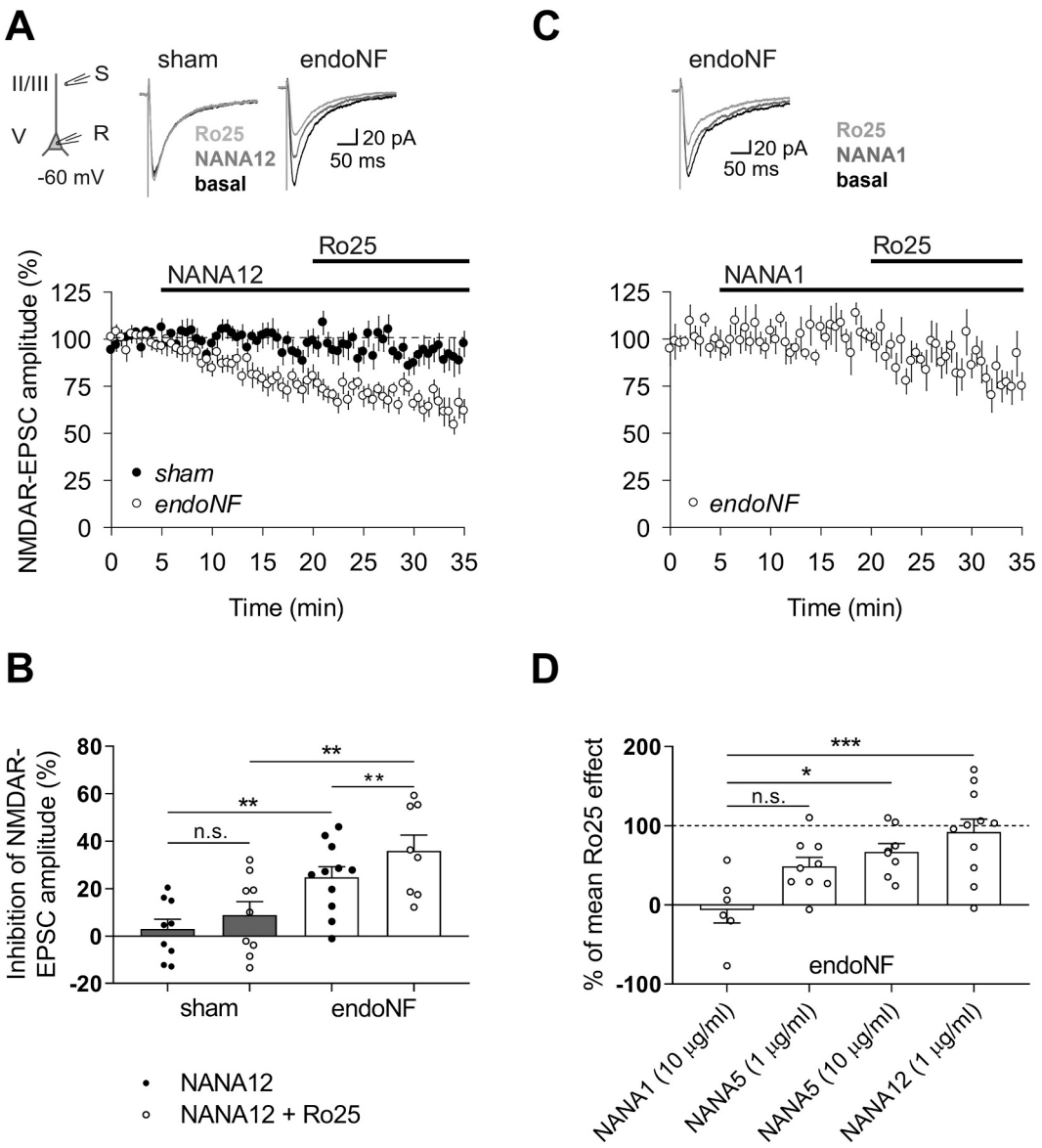

Fig. 3. Effects of polySia fragments on evoked NMDAR-EPSCs in endoNF-treated mPFC slices from C57BL/6J mice.
(A, C) Representative examples (top) and time courses of normalized amplitudes (bottom) of evoked NMDAR-EPSCs (holding potential −60 mV) during basal recording, followed by successive bath application of NANA12 (1 µg/ml) (A) or NANA1 (10 µg/ml, control compound) (C) and the GluN2B-subunit specific antagonist Ro 25–6981 (0.3 µM) in sham- and endoNF-treated slices. Note that NANA12 inhibited NMDAR-EPSCs in endoNF- but not in sham-treated slices. The experimental design in A and C was analogous to Fig. 1A, D.
(B) A bar graph summarizing mean inhibition levels of NMDAR-EPSC amplitude after NANA12 and NANA12 + Ro 25–6981 (cells presented in Fig. 3A). Two-way repeated measures ANOVA revealed significant effects of enzyme (sham/endoNF, $P < 0.001$) and drug treatment (NANA12 /NANA12 + Ro 25–6981, $P = 0.005$), and no enzyme x drug interaction ($P = 0.198$). $^{**}P < 0.01$, Holm-Sidak *post hoc* test. Inhibition of NMDAR-EPSC amplitude by NANA12 / NANA12 + Ro25 in sham / endoNF was analyzed during 10–15 min after their application, relative to baseline level (0–5 min). Numbers of cells recorded and mice used (n/N) are: NANA12 in sham group, 9/4; NANA12 + Ro25 in sham group, 9/4; NANA12 in endoNF group, 11/7; NANA12 + Ro25 in endoNF group, 8/6.
(C) No effect of NANA1 but a significant inhibition of NMDAR-EPSC amplitude by Ro 25–6981 in endoNF-treated slices.
(D) A bar graph summarizing effects of NANA1, NANA5, and NANA12 on NMDAR-EPSC amplitude in endoNF-treated slices (normalized to the mean Ro 25–6981-mediated inhibition of amplitude in endoNF slices shown in Fig. 1D, E). One-way ANOVA revealed a significant difference between treatment groups ($P = 0.0012$). $^{*}P < 0.05$, $^{***}P < 0.001$, Dunnett's *post hoc* test. Numbers of cells recorded and mice used (n/N) are: NANA1 group, 6/4; NANA5 (1 µg/ml) group, 9/6; NANA5 (10 µg/ml) group, 8/5; NANA12 group, 11/7. Data are shown as mean ± SEM.

results suggest that tegaserod does not act specifically on GluN2B-mediated synaptic transmission and thus does not mimic the effects of polySia on NMDARs.

3.4. Impaired LTP after endoNF treatment is restored by Ro 25–6981, NANA12, and sarcosine

To investigate whether a loss of polySia might affect synaptic plasticity in the prefrontal cortex, we recorded theta-burst stimulation (TBS)-induced LTP from layer II/III – layer V synapses in sham- and endoNF-treated mPFC slices from C57BL/6J mice. This form of LTP depends on NMDAR activation (Huang et al., 2004). The TBS induced stable LTP in mPFC of sham-treated slices; however, LTP was impaired in slices treated with endoNF (Fig. 4A, D). EndoNF- and sham-incubated slices exhibited similar relationships between stimulation intensity and fEPSP slope (Fig. S6A), indicating that the effects of polySia removal on

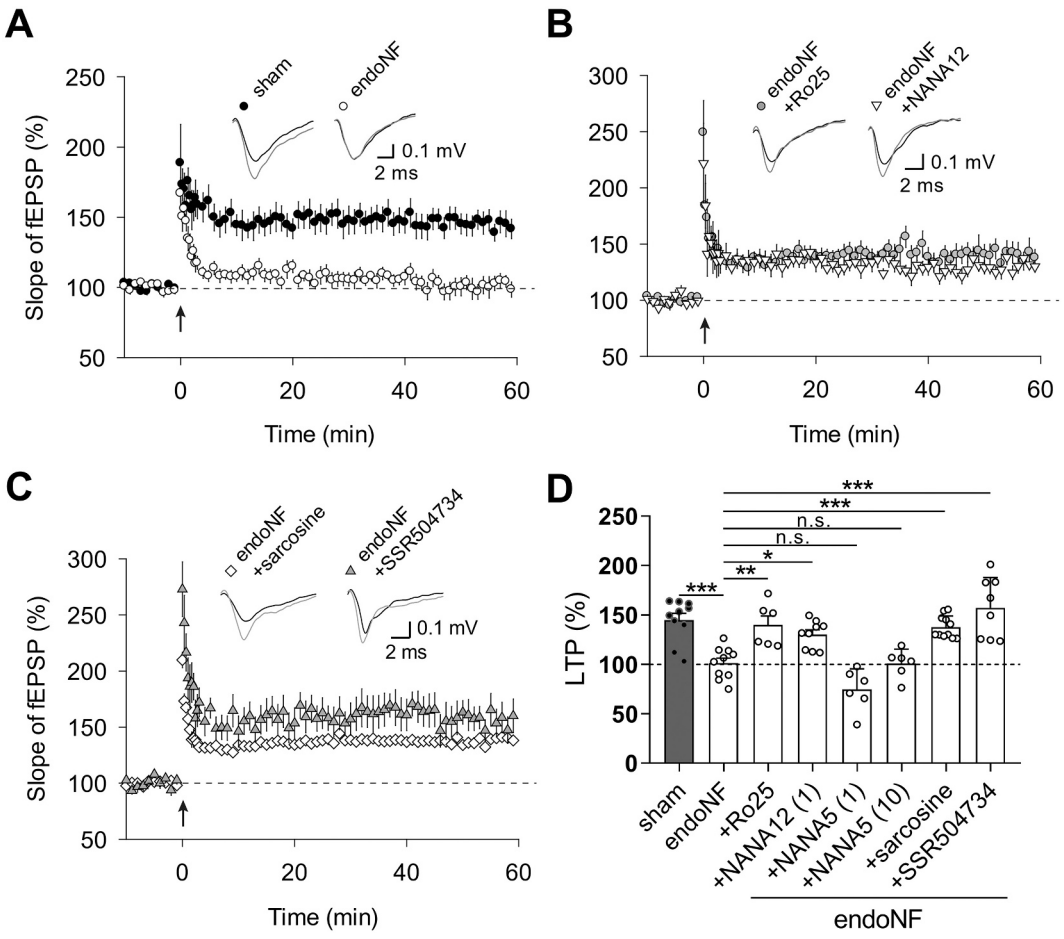

Fig. 4. Impact of endoNF, Ro 25–6981, polySia fragments, and GlyT1 inhibitors on LTP in mPFC slices.
(A) Time courses of the normalized mean slope of field excitatory postsynaptic potentials (fEPSPs) showing impaired TBS-induced LTP in endoNF- compared with sham-treated slices.
(A-C) Delivery of 5× TBS is indicated by arrows. Insets show averages of 30 fEPSPs recorded during 10 min before TBS (black) and 50–60 min after TBS (gray), respectively, in each condition. The mean slope of fEPSPs recorded 10 min before TBS was taken as 100%.
(B) Complete restoration of LTP levels in endoNF-treated slices when recorded in the presence of the GluN2B-selective antagonist Ro 25–6981 (0.3 μM) or NANA12 (1 μg/ml).
(C) Both glycine transporter type 1 inhibitors, sarcosine (0.75 mM) and SSR 504734 (3 μM), restored LTP magnitude in endoNF-treated slices to the level measured in sham-treated slices.
(D) A bar graph summarizing mean levels of LTP measured 50–60 min after TBS application in A–C. Note that NANA12 was tested at 1 μg/ml (1). NANA5 was tested at 1 μg/ml (1) and 10 μg/ml (10). One-way ANOVA revealed a significant difference between groups ($P < 0.001$). *$P < 0.05$, **$P < 0.01$, ***$P < 0.001$, Dunnett's *post hoc* test comparisons with endoNF-treated group. Data are shown as mean ± SEM.

LTP are not mediated by altered basal synaptic transmission.

Because our patch-clamp recordings revealed increased GluN2B-mediated transmission in endoNF slices (Fig. 1D–F) and similar inhibition of NMDAR-EPSCs by Ro 25–6981, NANA12, and NANA5 (Fig. 3D), we investigated whether these pharmacological treatments may rescue abnormal LTP by suppressing GluN2B-NMDARs. Field EPSP recordings revealed a full restoration of LTP levels in endoNF-treated slices perfused with Ro 25–6981 or NANA12 (Fig. 4B, D), indicating that NANA12 was as effective as Ro 25–6981 in restoring LTP. In sham-treated slices, we observed no effect of Ro 25–6981 on LTP magnitude (Fig. S6B), suggesting that GluN1/GluN2B-NMDARs do not contribute to LTP induction in the prefrontal cortex in our recording conditions. In contrast to NANA12, NANA5 (at 1 or 10 μg/ml) did not rescue LTP in endoNF-incubated slices (Fig. 4D). Notably, the application of NANA5 did not significantly change the mean fEPSP slope during baseline recordings (Fig. S6C). Since neither basal synaptic transmission nor LTP was affected by NANA5, we thus conclude that NANA5 has less potent inhibitory effects on GluN1/GluN2B receptors as compared to NANA12, and/or has side effects preventing induction of LTP.

Next, we explored the possibility that impaired LTP after endoNF treatment may be rescued by increasing synaptic NMDAR transmission with the clinically used glycine transporter type 1 (GlyT1) inhibitor sarcosine. Sarcosine elevates the glycine concentration in the synaptic cleft through inhibition of glycine reuptake by the GlyT1 (Harvey and Yee, 2013; Smith et al., 1992). Strikingly, in the presence of sarcosine, the LTP magnitude in endoNF-treated slices was fully restored to sham levels (Fig. 4C, D). In agreement with these data, another GlyT1 inhibitor, SSR 504734 (Depoortere et al., 2005), also rescued LTP in endoNF-treated slices (Fig. 4C, D).

3.5. Unaltered TBS-evoked IPSCs after endoNF treatment

In the mPFC, polySia was reported to be predominantly expressed in a subpopulation of interneurons (Gomez-Climent et al., 2011; Nacher et al., 2013); hence, a loss of polySia might promote GluN2B-mediated excitation of interneurons and thus impair LTP. To examine recruitment of cortical inhibitory interneurons by our TBS protocol, we isolated TBS-evoked inhibitory postsynaptic currents (IPSCs) by recording at the

reversal potential of EPSCs, *i.e.*, at 0 mV, in normal aCSF. The ratio between TBS-induced IPSC and basal EPSC amplitudes was similar in endoNF- and sham-treated slices (Fig. S7A-C), suggesting that the GABAergic inhibition of pyramidal cells is normal during the induction of LTP after polySia removal.

3.6. Increased GluN2B-mediated transmission and restoration of LTP in ST8SIA4-deficient mice

Because acute removal of polySia led to elevated synaptic transmission through GluN2B-NMDARs (Fig. 1D–F), we wondered whether this might also be the case in mice that are constitutively deficient in the polysialyltransferase ST8SIA4 (*St8sia4*$^{-/-}$) and that show no detectable polySia in the mPFC during adulthood (Eckhardt et al., 2000; Nacher et al., 2010). Whole-cell recordings from pyramidal cells revealed normal NMDAR/AMPAR current ratios in *St8sia4*$^{-/-}$ mice compared to their wild-type littermates (Fig. S8A). No difference in Ro 25–698-mediated inhibition of evoked NMDAR-EPSC amplitude was detected between *St8sia4*$^{-/-}$ and *St8sia4*$^{+/+}$ mice (Fig. 5A, B; for absolute values, see Fig. S8B, left), but the decay time of these EPSCs was markedly shortened by Ro 25–6981 in *St8sia4*$^{-/-}$ compared with *St8sia4*$^{+/+}$ mice (Figs. 5A, C, S8B, right). In line with our data obtained after acute polySia removal using endoNF, this finding suggests that GluN2B-mediated synaptic transmission is also elevated after genetic ablation of polySia.

Extracellular fEPSP recordings demonstrated a pronounced decrease in LTP magnitude (by ~40%) in *St8sia4*$^{-/-}$ mice compared with *St8sia4*$^{+/+}$ mice (Fig. 5D, H), which resembled the LTP deficits found in endoNF-treated slices (Fig. 4A, D). This result could be reproduced in an independent set of recordings on another setup (Fig. S8C).

Previous studies have shown that diffusion of presynaptically released glutamate to the extracellular space, and thus activation of extrasynaptic NMDARs, might be more pronounced at room temperature than at physiological temperature, given the temperature dependence of glutamate transporters (Asztely et al., 1997; Kullmann and Asztely, 1998). To test whether the extent of extrasynaptic NMDAR-mediated LTP reduction in *St8sia4*$^{-/-}$ mice would depend on recording temperature, we repeated LTP recordings in slices from *St8sia4*$^{-/-}$ mice and *St8sia4*$^{+/+}$ mice at 35 °C. In line with our recordings at room temperature, LTP levels in *St8sia4*$^{-/-}$ slices were significantly decreased (by ~40%) compared with *St8sia4*$^{+/+}$ mice (Fig. S8D). Moreover, the LTP magnitude in *St8sia4*$^{-/-}$ slices at 35 °C was similar to that measured at room temperature. These data indicate that the TBS-induced activation of extrasynaptic NMDARs is comparable at room *versus* physiological temperature.

In agreement with our endoNF data, we observed full restoration of LTP levels in mPFC slices from *St8sia4*$^{-/-}$ mice in the presence of either Ro 25–6981 (Fig. 5E, H), NANA12 (Fig. 5F, H), or sarcosine (Fig. 5G, H). Notably, Ro 25–6981, NANA12, and sarcosine had no effect on the LTP magnitude in *St8sia4*$^{+/+}$ mice (Fig. 5E–H), as shown for Ro 25–6981 in C57BL/6 J mice (Fig. S6B). These results indicate that resetting the balance between synaptic and extrasynaptic NMDAR activation may normalize synaptic plasticity in *St8sia4*$^{-/-}$ mice.

3.7. Normal synaptic plasticity in mice lacking ST8SIA2

During embryonic development, polySia is synthesized predominantly by the polysialyltransferase ST8SIA2 (Kröcher et al., 2015) and its deficiency affects thalamocortical connectivity as well as the development of GABAergic interneurons in the mPFC (Kröcher et al., 2015; Kröcher et al., 2014). To explore the relevance of ST8SIA2 for synaptic plasticity in the adult mPFC, we recorded TBS-induced LTP in mPFC slices from adult transgenic *St8sia2*$^{-/-}$ mice and their wild-type littermates. We measured comparable levels of LTP in *St8sia2*$^{-/-}$ and *St8sia2*$^{+/+}$ mice (Fig. 5I), indicating that polySia synthetized by ST8SIA2 is not involved in TBS-induced synaptic plasticity in the adult mPFC.

3.8. Impaired object recognition memory in polySia-deficient mice and its restoration by NANA12 and sarcosine

The prefrontal cortex is known to be involved in object recognition memory in rodents (Barbosa et al., 2013). A previous study revealed that *St8sia4*$^{-/-}$ mice are impaired in a novel object recognition task, when tested 2 h after encoding/familiarization phase (Kröcher et al., 2015). Hence, we subjected *St8sia4*$^{-/-}$ mice and their wild-type littermates to this paradigm (Fig. 6A, left) to evaluate the efficiency of treatments that restored synaptic plasticity in terms of their cognitive effects. Our data confirmed the defect in novel object recognition in *St8sia4*$^{-/-}$ mice, which spent equal time exploring familiar and novel objects in the test trial, while their *St8sia4*$^{+/+}$ littermates showed a preference for the novel object (Fig. 6B). On the next day, mice were i.p. injected with sarcosine or vehicle 30 min before the encoding phase (Fig. 6B). Then, sarcosine-treated *St8sia4*$^{-/-}$ mice reached the levels of object discrimination seen in control *St8sia4*$^{+/+}$ mice injected with either vehicle or sarcosine (Fig. 6B), suggesting that sarcosine could fully restore the impaired novel object recognition memory in mice lacking the polySia-synthesizing enzyme ST8SIA4.

Because LTP was impaired in mPFC slices treated with endoNF, we asked whether acute removal of polySia in the mPFC would affect learning and memory. Thus, we performed a longitudinal experiment comparing the performance of C57BL/6 J mice before and after endoNF injection into the mPFC *in vivo*, which efficiently digested polySia (Fig. S9A, B). Two days or one day prior to the administration of endoNF, mice showed normal object recognition after i.p. injection of either vehicle (at d-2) or sarcosine (at d-1) applied 30 min before the encoding phase (Fig. 6C). In contrast, one day after injection of endoNF into the mPFC (d1), the same mice were impaired in discriminating novel *versus* familiar objects (Fig. 6C). This deficit was fully alleviated by i.p. injection of sarcosine on day 2 (d2). Consistent with the short lifetime of sarcosine and the fact that the recovery of polySia expression lasts >1 week after a single endoNF injection (Seki and Rutishauser, 1998), impaired novel object recognition of the endoNF-treated mice was reinstated one day after the sarcosine injection (d3).

Because NANA12 rescued LTP *in vitro*, we also tested its effects *in vivo*. At day 5 (d5) NANA12 was applied intranasally 30 min before the encoding phase. NANA12 significantly improved novel object recognition, while intranasal administration of NANA1 on day 6 (d6) had no effect (Fig. 6C).

To verify that NANA12 penetrates into the brain after intranasal delivery, we applied NANA12 covalently coupled to a fluorescent dye, 1,2-diamino-4,5-methylenedioxybenzene.2HCl (DMB), and performed live two-photon imaging of DMB-NANA12 conjugates in the mPFC of *Thy1*-EGFP mice. The EGFP signal was used for finding the same position during repetitive imaging and for normalization of the DMB signal. We observed a rapid penetration of both DMB-NANA12 and the control reagent DMB-NANA2. Both could be detected 30 min after intranasal delivery, followed by a further increase in the DMB/EGFP signal ratio at 3 h and a decline at 24 h after the application (Fig. S9C).

Next, we attempted to rescue cognitive functions in *St8sia4*$^{-/-}$ mice by DMB-NANA12 delivery. Since we observed a positive effect of NANA12 in endoNF-treated mice with a 30-min interval between intranasal delivery and encoding phase (Fig. 6C), we continued to use this time interval in the following series of experiments. Consistent with data shown in Fig. 6B, C, another cohort of *St8sia4*$^{-/-}$ mice showed impaired novel object recognition, which was fully rescued by intranasal delivery of DMB-NANA12 but not by control DMB-NANA2 (Fig. 6D). To provide further evidence that NANA12 can rescue mPFC function, we examined the performance of *St8sia4*$^{-/-}$ mice using a recency (temporal order) task (Fig. 6A, right), in which healthy mice preferentially explore an object presented less recently, whereas impaired mice explore the recent (last) and less recent (second to last) object equally (Nelson et al., 2011). Lesion studies have shown that this temporal order memory task relies on the function of mPFC (Barker et al., 2007; Nelson et al., 2011).

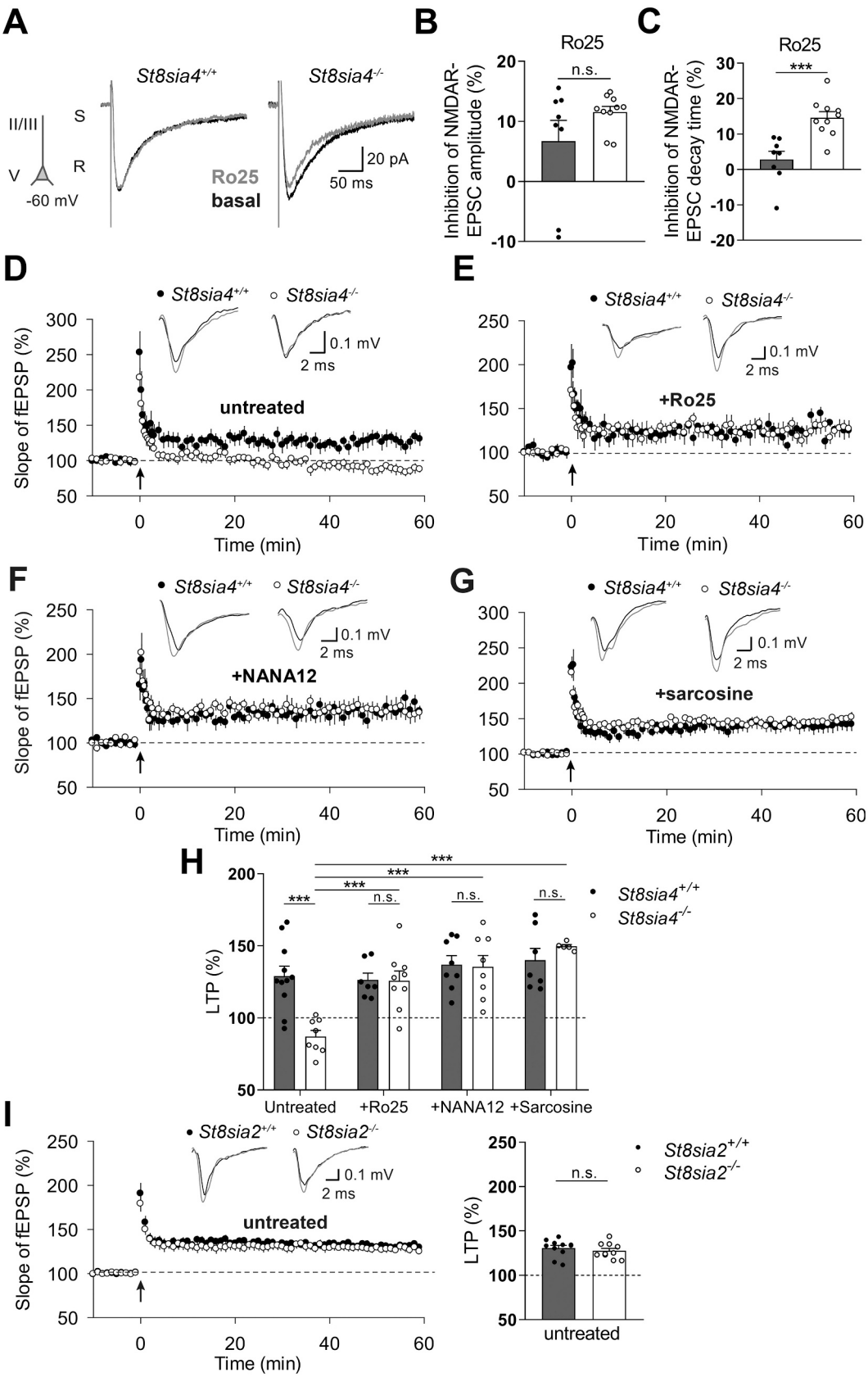

(caption on next page)

Fig. 5. GluN2B-NMDAR-mediated currents and restoration of LTP in the mPFC of ST8SIA4-deficient mice by Ro 25–6981, NANA12, and sarcosine.
(A) Representative examples of evoked NMDAR-EPSCs (holding potential −60 mV) before (basal, black) and after bath application of the selective GluN2B antagonist Ro 25–6981 (0.3 μM, gray) in mPFC pyramidal cells from *St8sia4*$^{-/-}$ mice and their *St8sia4*$^{+/+}$ littermates. NMDAR-EPSCs were recorded analogously to data in Fig. 1A (experimental design in inset).
(B, C) Bar graphs showing unchanged amplitude (B) and accelerated decay of NMDAR-EPSCs (C) upon Ro 25–6981 application in slices from *St8sia4*$^{-/-}$ mice compared with *St8sia4*$^{+/+}$ mice (***$P < 0.001$, unpaired Student's *t*-test).
(D) Time courses of normalized mean fEPSP slopes showing reduced levels of TBS-induced LTP in slices from *St8sia4*$^{-/-}$ mice compared with *St8sia4*$^{+/+}$ controls.
(E–G) Fully restored LTP levels in slices from *St8sia4*$^{-/-}$ mice and unchanged LTP levels in *St8sia4*$^{+/+}$ mice in the presence of Ro 25–6981 (0.3 μM) (E), short-chain polySia NANA12 (1 μg/ml) (F), and sarcosine (0.75 mM) (G).
(H) Summary of mean LTP levels in *St8sia4* mice in D–G. Two-way ANOVA revealed significant effects of genotype ($P < 0.03$) and treatment ($P < 0.001$), and a genotype x treatment interaction ($P = 0.001$). ***$P < 0.001$, Holm-Sidak *post hoc* test.
(I) Time courses of normalized mean fEPSP slope (left) and a bar graph (right) of LTP levels in *St8sia2*$^{-/-}$ and *St8sia2*$^{+/+}$ slices ($P = 0.443$, unpaired Student's *t*-test). Time courses of fEPSP slope and fEPSPs examples are presented analogously to Fig. 4. Bar graphs (H and I, right) show LTP levels measured 50–60 min after TBS. Numbers of cells (B, C) or slices (H, I) recorded are presented in bars. Data are shown as mean ± SEM.

St8sia4$^{+/+}$ mice showed a clear preference for the less as compared to the more recently explored object in the retrieval phase. In contrast, *St8sia4*$^{-/-}$ mice explored the two objects equally (Fig. 6E). Their performance in this task could be restored by DMB-NANA12 but not by the control compound DMB-NANA2, suggesting that recency memory depends, at least partially, on polySia availability.

3.9. Impaired mPFC LTP and recent object recognition memory in mice overexpressing AAV-Tau[R406W]-GFP are normalized by NANA12

Overexpression of mutant human Tau in mice is a model for dementia associated with upregulation of extrasynaptic GluN2B-mediated signaling (Li et al., 2011). We attempted to rescue synaptic and cognitive functions in mice injected with AAV-Tau[R406W]-GFP into the mPFC using AAV-GFP injection as a control (Fig. 7A). Immunohistochemical analysis showed a strong upregulation of Tau phosphorylation one month after injection of AAV-Tau[R406W]-GFP (Labus et al., 2021) as compared to mice injected with AAV-GFP (Fig. 7B). Electrophysiological fEPSP recordings in mPFC slices from AAV-Tau[R406W]-GFP-injected mice showed reduced levels of LTP, compared to control AAV-GFP-injected mice. However, in the presence of NANA12, the LTP level in AAV-Tau[R406W]-GFP-injected mice was restored to control levels, indicating that NANA12 could fully rescue LTP (Fig. 7C).

In the behavioral recency test, control AAV-GFP-injected mice showed a normal discrimination between more and less recently explored objects, while AAV-Tau[R406W]-GFP-injected mice displayed impaired recent object recognition. This cognitive phenotype was fully rescued by intranasal delivery of NANA12, but not by control NANA1 (Fig. 7D).

3.10. Impaired recent object recognition memory in 5xFAD mice is normalized by NANA12

Next, we investigated the effect of NANA12 on cognition in a second mouse model of dementia using 5xFAD mice, a model of amyloidosis in familial Alzheimer's disease. A previous analysis of extrasynaptic NMDAR-mediated currents in the cortex of adult 5xFAD mice revealed no changes in the amplitude but an increase in the deactivation time constant, suggesting an increase in the contribution of slowly deactivating GluN2B-containing NMDARs (Back et al., 2021) like we found here for St8Sia4$^{-/-}$ mice. Moreover, Aβ inhibits reuptake of synaptically released glutamate and increases concentration of perisynaptic glutamate (Zott et al., 2019). Hence, amyloidosis promotes activation of extrasynaptic GluN2B-containing NMDARs, which we aimed to inhibit by NANA12.

First, we established that 13- to 14-month-old 5xFAD mice are impaired in recency memory, when tested after a 90 min intertrial interval between the two encoding phases. In contrast to age-matched littermates, 5xFAD mice showed no discrimination between objects during recall and spent the same time near the more recently and the less recently explored objects (Fig. 7E, left panels). To test whether application of NANA12 is able to improve cognitive function in the 5xFAD model, NANA12 or vehicle (H_2O) were intranasally delivered. Each mouse received both drugs and vehicle, in a random order and separated by 4 days. According to the measured time-course of NANA12 delivery to the brain (see Fig. S9), the recency test was started 2 h after drug delivery, *i.e.* at the estimated peak of drug concentration in the mPFC, and a concentration of 0.5 mg/kg was applied. In contrast to the vehicle-treated group, 5xFAD mice that received NANA12 showed a clear preference for the less recently as compared to the more recently explored object in the retrieval phase (Fig. 7E, right panels).

4. Discussion

Our data demonstrate that polySia controls the balance of signaling through synaptic *versus* extrasynaptic NMDA receptors in the mPFC, the region in which structural changes have been associated with an increased concentration of serum polySia in schizophrenic patients. Enzymatic or genetic ablations of polySia expression in endoNF-treated wild-type and *St8Sia4*$^{-/-}$ mice, respectively, lead to elevation of GluN1/GluN2B-mediated evoked and tonic extrasynaptic currents, and impairments in mPFC LTP, as well as in novel and recent object recognition memories. These results and the normal mPFC LTP in *St8Sia2*$^{-/-}$ mice are consistent with previous analysis of LTP in the CA1 region of the hippocampus and the known differences in the temporal expression of these enzymes (Hildebrandt and Dityatev, 2015): expression of ST8SIA2 peaks during early development while ST8SIA2 is the major polysialyltransferase in the mature brain. Accordingly, there are detectable changes in polySia immunoreactivity in the mPFC of *St8Sia2*$^{-/-}$ mice, whereas *St8Sia4*$^{-/-}$ mice show abolished polySia expression in the mPFC (Nacher et al., 2010). Reintroduction of short polySia fragments, or resetting the balance between synaptic GluN2A- *versus* extrasynaptic GluN2B-mediated transmission by Ro25–6981 or sarcosine, restored LTP, object recognition, and recency memory in polySia-deficient mice (for a model, see Fig. 8). These data suggest that sarcosine or newer, more potent GlyT1 inhibitors will be particularly efficient to normalize cognitive functions of schizophrenia patients with dysregulated levels of serum polySia. It is plausible that also dementia patients with elevated levels of serum polySia may benefit from such treatment. We anticipate that our work will stimulate verification of this prediction in clinical settings. To assess the function of predominantly extrasynaptic heterodimeric GluN1/GluN2B receptors, we used low concentration of Ro 25–6981 (Volianskis et al., 2013) (France et al., 2017), which has a ~ 25times higher potency in blocking GluN2B-NMDARs than ifenprodil (Fischer et al., 1997). Moreover, the present study targeted the activity of extrasynaptic NMDARs by using the polySia, which inhibited GluN2B activation by glutamate at an extrasynaptic-like (3 μM) glutamate concentration. We show that depleting polySia using endoNF increased the contribution of 0.3 μM Ro 25–6981- and NANA12-sensitive NMDAR currents and increased tonic NMDAR currents. Cumulatively, these data suggest that the activity of extrasynaptic NMDARs is elevated after polySia depletion, which is accompanied by decreased LTP levels in the

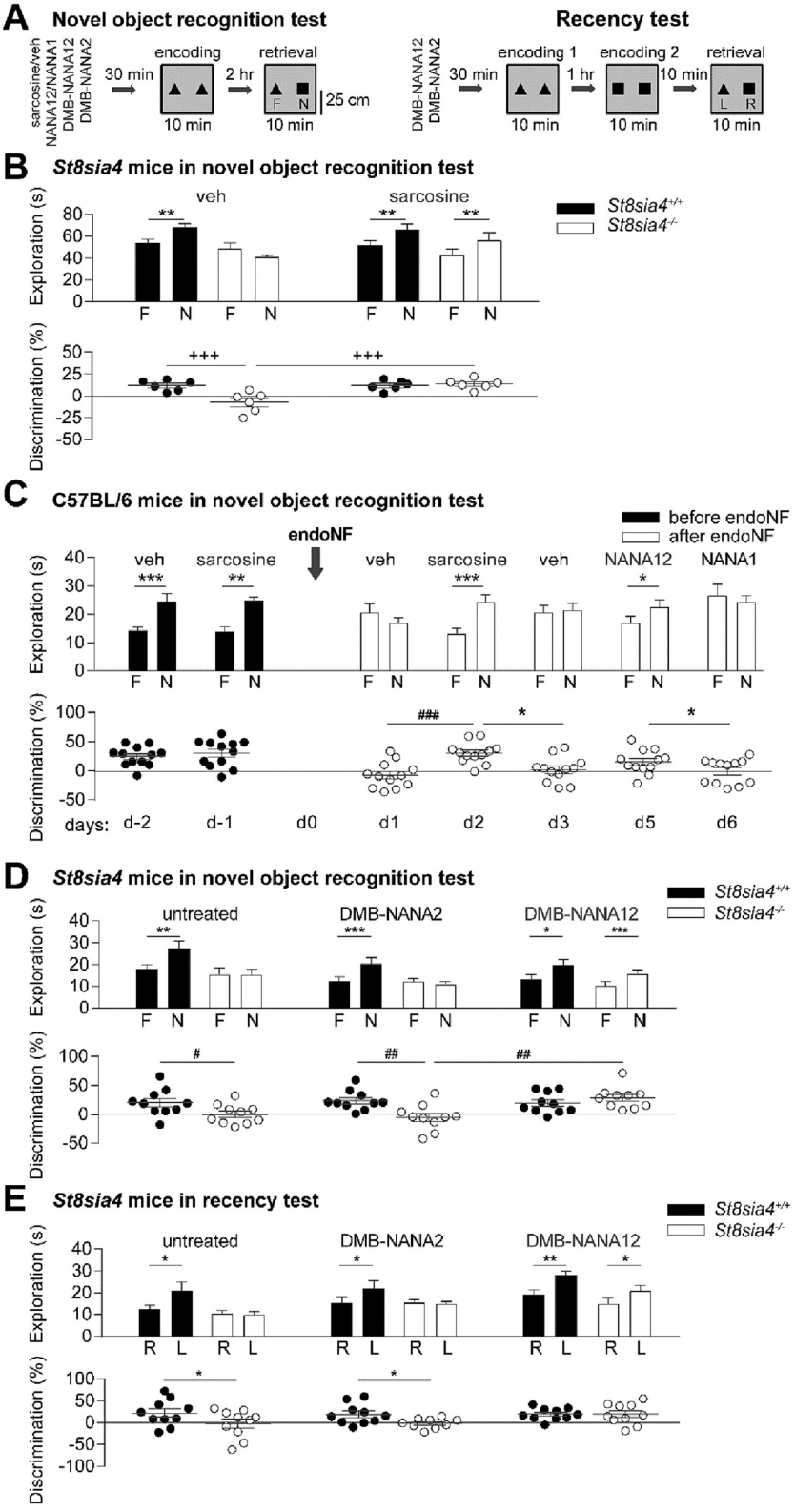

Fig. 6. Novel object recognition and recency tests in *St8sia4*$^{-/-}$ mice and after *in vivo* intra-mPFC injection of endoNF in C57BL/6J mice.

(A) Experimental design of novel object recognition test and recency test. In the novel object recognition test, sarcosine (600 mg/kg, intraperitoneally), NANA12 / NANA1 (1 mg/kg, intranasally), and DMB-NANA12 / DMB-NANA2 (2 mg/kg, intranasally) were delivered 30 min before the encoding phase, and retention of memory was evaluated 2 h later, in the retrieval phase. In the recency test, reagents were applied 30 min before the first of two encoding phases at 1-h interval, and recency memory was then assessed 10 min later.

(B-E) Upper panels show exploration times, while lower panels show discrimination ratio (%) in all tested groups and trials.

(B) Rescue of *St8sia4*$^{-/-}$ *mice* performance by sarcosine. *St8sia4*$^{+/+}$ mice (n = 6) spent significantly longer time exploring new objects (N) *versus* familiar objects (F), and sarcosine did not improve their performance. However, *St8sia4*$^{-/-}$ mice (n = 6) failed to show a preference for novel objects, and sarcosine could rescue this cognitive impairment. $^{**}P < 0.01$, paired Student's *t*-test. Two-way repeated measures ANOVA (lower panel in B) revealed significant effects of genotype ($P = 0.022$), sarcosine treatment ($P = 0.008$) in *St8sia4*$^{-/-}$ mice, and a significant genotype x treatment interaction ($P = 0.008$). $^{+++}P < 0.001$, Holm-Sidak *post hoc* test.

(C) Exploration time and object discrimination ratio before and after intra-mPFC endoNF injection in C57BL/6J mice ($n = 12$). An arrow shows the timing of endoNF injection. Novel object recognition is impaired on day 1 and 3 after endoNF intra-mPFC injection, but it can be rescued by sarcosine at day 2. Intranasal delivery of NANA12 at day 5 could also restore cognitive function compared to the control compound NANA1 at day 6. $^{*}P < 0.05$, $^{**}P < 0.01$, $^{***}P < 0.001$, paired Student's *t*-test. Two-way repeated measures ANOVA for discrimination ratios on d-2, d-1, d1, and d2 (lower panel in C) showed statistically significant effects of endoNF injection ($P = 0.015$), sarcosine treatment ($P = 0.017$), and a significant endoNF x sarcosine interaction ($P = 0.002$). $^{\#}P < 0.05$, $^{\#\#\#}P < 0.001$, Holm-Sidak *post hoc* test; $^{*}P < 0.05$, paired Student's *t*-test.

(D, E) Rescue of *St8sia4*$^{-/-}$ mice ($n = 10$) performance in novel object recognition (D) and recency (E) tasks by DMB-NANA12. Untreated *St8sia4*$^{-/-}$ mice (n = 10) failed to discriminate between novel and familiar objects (D) as well as between the most recent (R) and least recent (L) objects (E). Intranasal administration of DMB-NANA12, but not of DMB-NANA2, restored cognitive function in *St8sia4*$^{-/-}$ mice in both tests. $^{*}P < 0.05$, $^{**}P < 0.01$, $^{***}P < 0.001$, paired Student's *t*-test. Two-way repeated measures ANOVA for discrimination ratio (lower panel in D) revealed statistically significant effects of genotype ($P = 0.005$) and a significant genotype x treatment interaction ($P = 0.017$). $^{\#}P < 0.05$, $^{\#\#}P < 0.01$, Holm-Sidak *post hoc* test. Data are shown as mean ± SEM.

mPFC. These data obtained in the mPFC are in line with studies in the CA1 region, where LTP is promoted only by synaptic, but not by extrasynaptic NMDARs, while LTD requires both fractions of NMDARs (Kochlamazashvili et al., 2012; Kochlamazashvili et al., 2010; Papouin et al., 2012).

To upregulate the function of synaptic NMDARs, we mostly used sarcosine because several clinical studies indicated that GlyT1 inhibitors might improve negative and cognitive symptoms in schizophrenia (Curtis, 2019), and sarcosine was among the most efficient drugs (Javitt, 2012). Functional activation of NMDARs requires the simultaneous binding of glutamate and its co-agonists glycine or D-serine (Balu and Coyle, 2015; Henneberger et al., 2010; Johnson and Ascher, 1987).

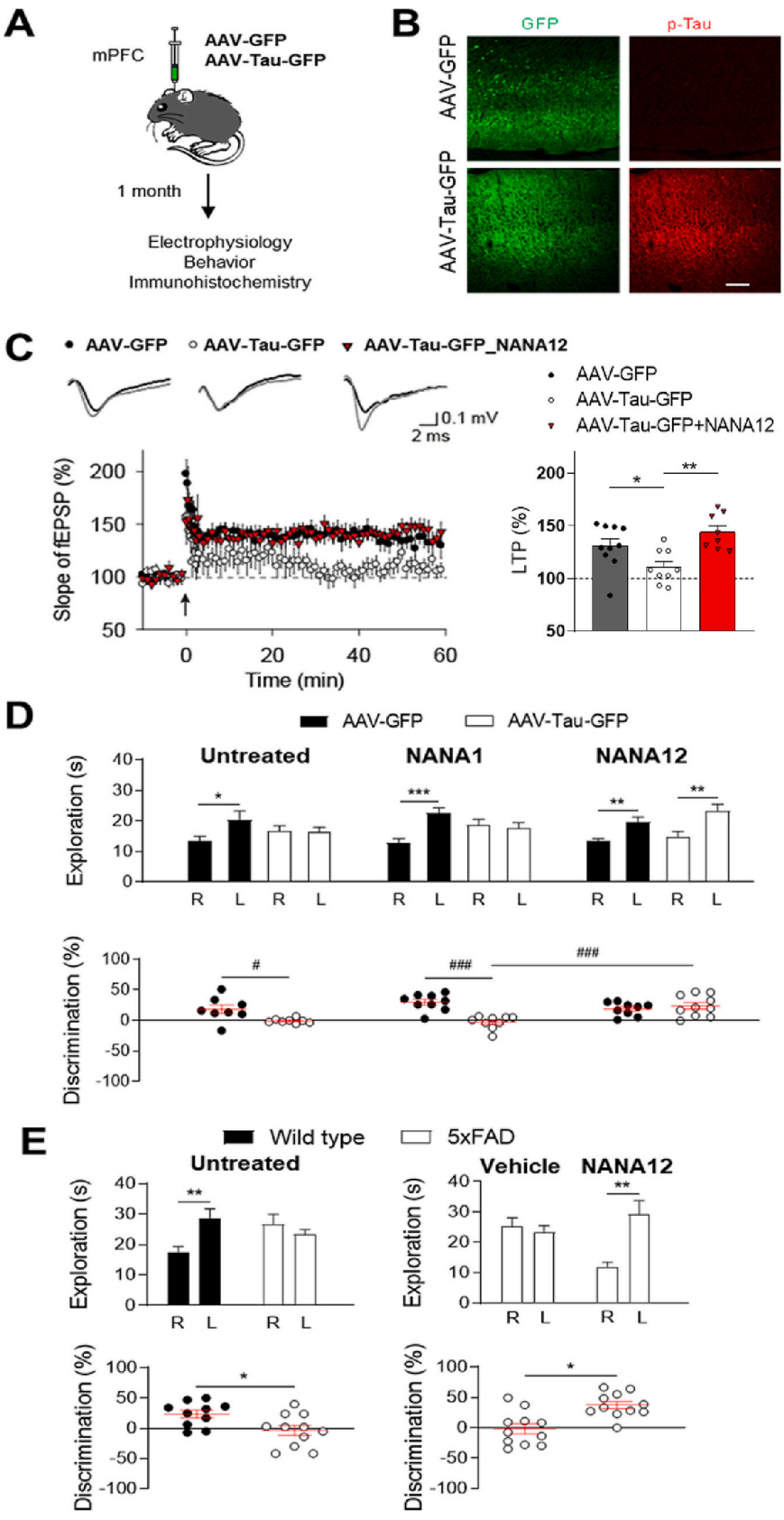

Fig. 7. NANA12 rescues mPFC LTP and recency memory in mouse models of dementia associated with tauopathy or amyloidosis.

(A) Schematic illustration showing the time plan of stereotaxic injections of AAVs into the mPFC, electrophysiological fEPSP recordings in mPFC, behavioral recency test, and immunohistochemistry in AAV-Tau-GFP- and AAV-GFP-injected mice, in B–D.

(B) AAV-driven expression of Tau[R406W]-GFP (AAV-Tau-GFP) and control GFP (AAV-GFP) in the medial prefrontal cortex, 1 month after stereotaxic injection of AAVs. Expression of Tau[R406W]-GFP leads to increased level of phosphorylated Tau (p-Tau). Scale bar, 100 μm.

(C) Injection of AAV-Tau-GFP results in impaired mPFC LTP, which could be rescued by application of NANA12 at 1 μg/ml (≈ 0.3 μM). Inserts above LTP profiles show representative traces for fEPSPs recorded 10 min before and 50–60 min after induction of LTP. The bar plot depicts mean ± SEM values of LTP 50–60 min after induction. One-way ANOVA revealed a significant difference between groups ($P = 0.003$). $^{*}P < 0.05$, $^{**}P < 0.01$, Dunnett's *post hoc* test for comparisons with AAV-Tau-GFP-treated group.

(D) Rescue of performance of AAV-Tau[R406W]-GFP-injected mice (n = 10) in the recency test by NANA12. Untreated AAV-Tau[R406W]-GFP-injected mice failed to discriminate the most recent (R) and least recent (L) objects, in contrast to AAV-GFP injected mice ($n = 9$). Intranasal administration of NANA12, but not of NANA1, restored cognitive function in the recency test. $^{*}P < 0.05$, $^{**}P < 0.01$, $^{***}P < 0.001$, paired Student's *t*-test. Two-way repeated measures ANOVA for discrimination ratio revealed statistically significant effects of Tau ($P = 0.0003$), treatment ($P = 0.0205$) and a significant Tau x treatment interaction ($P = 0.0001$). $^{\#}P < 0.05$, $^{\#\#\#}P < 0.001$, Holm-Sidak *post hoc* test. Data are shown as mean + SEM values.

(E) Impaired performance of 5xFAD mice ($n = 11$) in the recency test, in contrast to normal performance in control wild-type mice (n = 10) ($^{**}P < 0.01$, paired Student's *t*-test). Discrimination ratio was significantly lower in untreated 5xFAD mice, as compared to wild-types ($^{*}P < 0.05$, paired Student's *t*-test). Another batch of NANA12-injected 5xFAD mice (6 male and 5 female) showed restored discrimination between more recent (R) and less recent (L) objects, in contrast to vehicle-injected 5xFAD mice ($^{**}P < 0.01$, paired Student's *t*-test). One-way repeated measures ANOVA for discrimination ratio revealed statistically significant difference between treatments ($P = 0.012$). $^{*}P < 0.05$, *post hoc* Holm-Sidak test for comparison between vehicle and NANA12. Data are shown as means ± SEM.

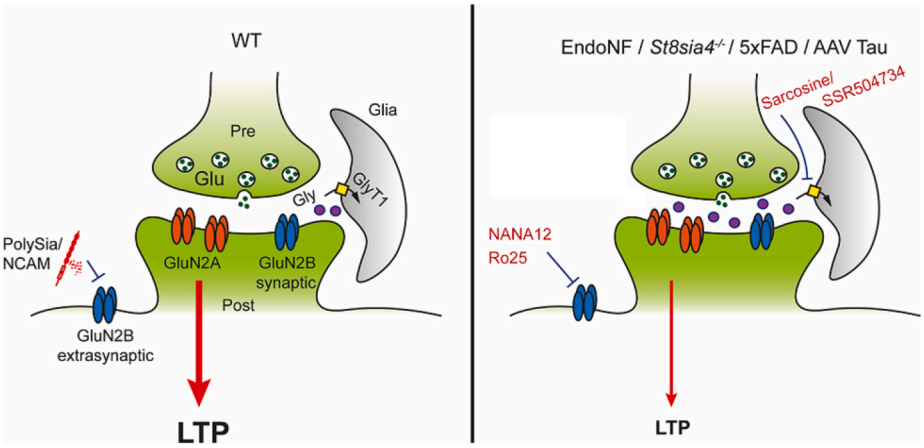

Fig. 8. A model of polySia-NCAM-mediated modulation of NMDARs at excitatory glutamatergic synapses in the mouse mPFC.
Left: In the mPFC of wild-type (WT) mice, polySia-NCAM inhibits membrane currents through GluN2B-containing NMDARs that are located extrasynaptically and are activated by low concentrations of glutamate. Under this condition, normal LTP is mainly promoted through GluN2A-containing synaptic NMDARs. Note that the glial glycine transporter 1 (GlyT1) is responsible for reuptake of glycine (gly), which results in a relatively low glycine concentration in the vicinity of postsynaptic NMDARs.
Right: Under conditions of polySia deficiency following its acute enzymatic (endoNF) or genetic abrogation (*St8sia4*$^{-/-}$ mice), evoked and tonic currents through extrasynaptic GluN1/GluN2B-containing NMDARs are increased, while currents through synaptic NMDAR are decreased, leading to a marked decrease in mPFC LTP. This impairment could be fully restored to wild-type levels by resetting the synaptic to extrasynaptic NMDAR ratio using i) low concentrations of the GluN2B-NMDAR-specific antagonist Ro 25–6981 (Ro25), ii) the short-chain polySia NANA12, iii) the glycine transporter 1 inhibitors sarcosine and SSR 504734. NANA12 also rescued synaptic plasticity and learning in 5xFAD mice after overexpression of Tau protein by targeting overactivated extrasynaptic GluN2B receptors. Pre, presynapse; Post, postsynapse; Glu, glutamate.

NMDARs containing the GluN2B subunit have 10-fold higher affinity for glycine than those containing GluN2A (Paoletti et al., 2013). Hence, ambient levels of glycine/D-serine may saturate the NMDAR glycine binding site at extrasynaptic GluN2B but not at synaptic GluN2A-containing receptors (Javitt, 2012). Accordingly, sarcosine has no effect on tonic currents mediated by extrasynaptic NMDARs (Le Meur et al., 2007). Thus, our findings suggest that sarcosine rescues impaired mPFC LTP by activation of synaptic rather than extrasynaptic NMDARs.

Our data showing changes in LTP and the NMDAR subunit contribution in cortical pyramidal neurons are in line with a study, in which polySia removal reduced the dendritic spine density of pyramidal neurons and decreased neuropil expression of the excitatory synapse marker vesicular glutamate transporter-1 in the adult mPFC. In the perisomatic region of mPFC pyramidal neurons, endoN treatment, however, led to elevated density of inhibitory glutamic acid decarboxylase (GAD)65/67-positive as well as parvalbumin-positive puncta, while in the peridendritic region of mPFC pyramidal neurons, endoNF did not change the density of GAD65/67-expressing puncta (Castillo-Gomez et al., 2011). Further, genetic ablation of the polysialyltransferase ST8SIA4 led to a reduced complexity of the dendritic arbors of parvalbumin-expressing mPFC interneurons and to decreased density of parvalbumin-expressing perisomatic puncta on mPFC pyramidal neurons (Curto et al., 2019). Thus, these data with long-term deficit in polySia strongly suggest that polySia is involved in the control of perisomatic innervation of cortical pyramidal neurons by GABAergic interneurons. Our data demonstrate that TBS-elicited perisomatic inhibition of pyramidal cells was not modified after acute endoNF treatment, suggesting that polySia is not critical for acute physiological modulation of GABAergic transmission, but further experiments would be needed to evaluate GABAergic transmission and its modulation by NANA12 in conditions of chronic polySia deficiency and AD models.

In cultured hippocampal neurons, the addition of soluble polySia inhibited GluN2B-mediated NMDARs, whereas enzymatic removal of polySia had no effect on GluN2B-mediated currents (Hammond et al., 2006a). These data suggested that GluN2B-containing NMDARs might be altered only by soluble polySia and polySia-NCAM but not by polySia attached to NCAM at the neuronal cell surface (Hammond et al., 2006a). In mPFC slices, we found that endoNF increased GluN2B-mediated transmission to pyramidal cells, indicating that this effect is mediated by soluble polySia-NCAM stabilized in the extracellular space in slices, whereas in cultures, soluble polySia may readily diffuse to the culture medium and, therefore, be inefficient. The soluble form of polySia-NCAM can be produced after shedding of transmembrane NCAM by the metalloproteases of the disintegrin and a metalloprotease family ADAM10 or ADAM17 (Hinkle et al., 2006; Kalus et al., 2006).

As interneurons express most of the polySia produced by ST8SIA4 in the PFC (Brennaman et al., 2013; Gomez-Climent et al., 2011; Nacher et al., 2013; Nacher et al., 2010), the effects on pyramidal neurons might be mediated by polySia derived from interneurons. This is highly reminiscent of Reelin, which is synthesized by Cajal-Retzius cells and cortical interneurons (Alcantara et al., 1998) and promotes synaptic plasticity by acting on cognate receptors on pyramidal neurons that support the activity of synaptic NMDARs (Beffert et al., 2005; Dityatev et al., 2010). Reelin-haploinsufficient mice show impaired LTP and abnormal loss of fear memories. This phenotype is rescued by Ro 25–6981 (Iafrati et al., 2014), which is consistent with the concept that balancing synaptic/extrasynaptic signaling is the key to controlling synaptic plasticity. Thus, we hypothesize that in addition to the NMDAR-mediated influence of excitatory neurons on development and activity of interneurons (Belforte et al., 2010; Hardingham and Do, 2016), there are important feedback mechanisms. Interneurons may signal through secreted Reelin and shed polySia-NCAM to control the activity of synaptic and extrasynaptic NMDARs on pyramidal cells. Disruption of these feedback mechanisms may be linked to schizophrenia and dementia (Varbanov and Dityatev, 2017). Further dissection of the roles played by polySia synthetized by principal cells *versus* interneurons, *e.g.*, by conditional ablation of *St8Sia4* or the polySia-NCAM shedding enzyme(s) in these cell types, is warranted in follow-up studies.

Previously, we have shown that injection of a mixture of sialic acid polymers can rescue hippocampal LTP in NCAM-deficient mice (Senkov et al., 2006). To the best of our knowledge, the present study is the first to demonstrate the efficacy of a short, defined-length fragment of polySia (NANA12) for improvements of cortical synaptic and cognitive functions. We also show the advantages of NANA12 compared with sialic acid, the oligomer NANA5, or compared with the polySia mimetic tegaserod. Our experiments show that NANA5 has >10 times less potent inhibitory effects on GluN2B-containing receptors as compared to NANA12 and does not support induction of LTP even in 10 times higher concentration than NANA12. It is likely that due to its longer size, NANA12 has multiple binding sites, *i.e.* has a higher avidity to NMDARs than NANA5. As polySia dysregulation has been associated with

schizophrenia, epilepsy, AD, and regeneration (Barbeau et al., 1995; Gilabert-Juan et al., 2012), our study opens a new avenue for causal therapeutic treatment of these conditions by intranasal delivery of NANA12. Noteworthy, a deficit in polySia in AD was observed specifically in the entorhinal cortex (Murray et al., 2016). Since the mechanism of polySia action on NMDA receptors appears to be common for the hippocampus and prefrontal cortex, we expect that GlyT1 inhibitors and small polySia fragments, which we found to rescue synaptic plasticity in polySia-deficient prefrontal cortex, would also be effective in the entorhinal cortex. Furthermore, a deficit in polysialic acid in AD correlated with hyperphosphorylated Tau levels (Murray et al., 2016). As Tau accumulations are also commonly found in the cortex of patients with frontotemporal dementia and other tauopathies, and their neurotoxicity/cognitive effects are mediated by NMDARs (Amadoro et al., 2006; Decker et al., 2016; Tackenberg and Brandt, 2009), it is plausible that NANA12 has a potential to be used for treatment of these conditions. Further studies should directly evaluate the extend of inhibition of extrasynaptic GluN2B-containing NMDARs by NANA12 in models of tauopathy and amyloidosis. The efficacy of polySia fragments to rescue synaptic and cognitive functions was superior to that of clinically used sarcosine as much lower concentrations of polySia were necessary. Considering the important role of polySia in neural development, it is also likely that chronic NANA12 delivery may reactivate developmental forms of neuroplasticity and be efficient also for treatment of neurodevelopmental disorders.

The use of animal models in the current study provided new mechanistic insights, supporting the link between polySia and prefrontal cortex-dependent cognitive disturbances, which, however, remain to be translated into patient-related research. The present study demonstrates that small polySia fragments are highly efficient in multiple animal models and sufficient to mimic the synaptic and cognitive functions of complex glycoprotein polySia-NCAM. As polySia is endogenously synthetized in the brain, it is likely that food supplements or drugs including polySia fragments will be non-toxic and hence highly attractive for further development to control the balance in signaling mediated by the synaptic and extrasynaptic NMDARs.

Funding

This work has been supported by the Italian Institute of Technology and DZNE (to A.D.), the European Union's Horizon 2020 Research and Innovation Programme under the Marie Sklodowska-Curie grant agreement no. 642881 (ECMED; to A.D.), DFG SFB 1436 TP A03 (Project-ID 425899996) to A.D., NIH-R01 DA046723–01 to V.S., DFG grant GE801/17–1 to R.G.S. and BMBF project number 16LW0207 to H. T. W.S. has been supported by the State Scholarship Fund of the China Scholarship Council (grant number 201406170032).

Author contributions

H.V. performed most of the *in vitro* experiments and data analysis and wrote a draft of manuscript, G.K., and H.Ha. performed *in vitro* experiments and data analysis, S.J. developed intranasal NANA12 delivery, S. J. and M.T. performed behavioral experiments and data analysis, S.S., S. J. and W.S. performed *in vivo* imaging and data analysis, I.R., H.T., H.Hi. and R.G.-S. provided unique reagents and mouse lines and wrote the manuscript, O.S. supervised collection and analysis of behavioral data and wrote the manuscript, S.B., M.A.B., V.S. performed electrophysiological channel experiments, analyzed data, wrote related sections of the manuscript, and A.D. designed the study, supervised *in vitro* analysis, and wrote the manuscript.

CRediT authorship contribution statement

Hristo Varbanov: Methodology, Investigation, Formal analysis, Writing – original draft, Visualization. **Shaobo Jia:** Methodology, Investigation, Formal analysis, Writing – original draft, Visualization. **Gaga Kochlamazashvili:** Investigation, Formal analysis, Writing – original draft, Visualization. **Subhrajit Bhattacharya:** Investigation, Formal analysis, Writing – original draft, Visualization. **Manal Ali Buabeid:** Investigation, Formal analysis, Writing – original draft, Visualization. **Mohamed El Tabbal:** Investigation, Formal analysis, Writing – original draft, Visualization. **Hussam Hayani:** Investigation, Formal analysis, Writing – original draft, Visualization. **Stoyan Stoyanov:** Investigation, Formal analysis, Writing – original draft, Visualization. **Weilun Sun:** Investigation, Formal analysis, Writing – original draft, Visualization. **Hauke Thiesler:** Resources, Methodology, Writing – review & editing, Funding acquisition. **Iris Röckle:** Resources, Methodology, Writing – review & editing. **Herbert Hildebrandt:** Resources, Methodology, Writing – review & editing. **Oleg Senkov:** Methodology, Formal analysis, Supervision, Writing – original draft. **Vishnu Suppiramaniam:** Conceptualization, Resources, Writing – review & editing, Supervision, Funding acquisition. **Rita Gerardy-Schahn:** Conceptualization, Resources, Writing – review & editing, Supervision, Funding acquisition. **Alexander Dityatev:** Conceptualization, Resources, Writing – original draft, Supervision, Project administration, Funding acquisition.

Declaration of Competing Interest

H.V., A.D., S.J., R.G., and H·H. have filed an international patent application on "Polysialic acid and derivatives thereof, pharmaceutical composition and method of producing polysialic acid", WO2020025653A2.

Data availability

Data will be made available on request.

Acknowledgments

We thank Jenny Schneeberg and Katrin Boehm for excellent technical assistance, Dr. Inseon Song for helpful discussions of patch-clamp recordings, Dr. Rahul Kaushik for helpful discussions of immunohistochemistry, Maura Ferrer for help with spine imaging, Dr. Pierre Paoletti for the GluN1 expression vector, Dr. Evgeni Ponimaskin for AAV-GFP and AAV-Tau[R406W]-GFP, and Dr. Eckart Gundelfinger for provided lab space and support. We thank Thomas Frodl, Michael Kreutz, and Jakob von Engelhardt for valuable comments on the manuscript.

Appendix A. Supplementary data

Supplementary data to this article can be found online at https://doi.org/10.1016/j.nbd.2023.106079.

References

Alcantara, S., Ruiz, M., D'Arcangelo, G., Ezan, F., de Lecea, L., Curran, T., Sotelo, C., Soriano, E., 1998. Regional and cellular patterns of reelin mRNA expression in the forebrain of the developing and adult mouse. J. Neurosci. 18, 7779–7799.

Amadoro, G., Ciotti, M.T., Costanzi, M., Cestari, V., Calissano, P., Canu, N., 2006. NMDA receptor mediates tau-induced neurotoxicity by calpain and ERK/MAPK activation. Proc. Natl. Acad. Sci. U. S. A. 103, 2892–2897.

Asztely, F., Erdemli, G., Kullmann, D.M., 1997. Extrasynaptic glutamate spillover in the hippocampus: dependence on temperature and the role of active glutamate uptake. Neuron 18, 281–293.

Back, M.K., Ruggieri, S., Jacobi, E., von Engelhardt, J., 2021. Amyloid beta-mediated changes in synaptic function and spine number of neocortical neurons depend on NMDA receptors. Int. J. Mol. Sci. 22, 6298.

Balu, D.T., Coyle, J.T., 2015. The NMDA receptor 'glycine modulatory site' in schizophrenia: D-serine, glycine, and beyond. Curr. Opin. Pharmacol. 20, 109–115.

Barbeau, D., Liang, J.J., Robitalille, Y., Quirion, R., Srivastava, L.K., 1995. Decreased expression of the embryonic form of the neural cell adhesion molecule in schizophrenic brains. Proc. Natl. Acad. Sci. U. S. A. 92, 2785–2789.

Barbosa, F.F., Santos, J.R., Meurer, Y.S., Macedo, P.T., Ferreira, L.M., Pontes, I.M., Ribeiro, A.M., Silva, R.H., 2013. Differential cortical c-Fos and Zif-268 expression

after object and spatial memory processing in a standard or episodic-like object recognition task. Front. Behav. Neurosci. 7, 112.
Barker, G.R., Bird, F., Alexander, V., Warburton, E.C., 2007. Recognition memory for objects, place, and temporal order: a disconnection analysis of the role of the medial prefrontal cortex and perirhinal cortex. J. Neurosci. 27, 2948–2957.
Becker, C.G., Artola, A., Gerardy-Schahn, R., Becker, T., Welzl, H., Schachner, M., 1996. The polysialic acid modification of the neural cell adhesion molecule is involved in spatial learning and hippocampal long-term potentiation. J. Neurosci. Res. 45, 143–152.
Beffert, U., Weeber, E.J., Durudas, A., Qiu, S., Masiulis, I., Sweatt, J.D., Li, W.P., Adelmann, G., Frotscher, M., Hammer, R.E., Herz, J., 2005. Modulation of synaptic plasticity and memory by Reelin involves differential splicing of the lipoprotein receptor Apoer2. Neuron 47, 567–579.
Belforte, J.E., Zsiros, V., Sklar, E.R., Jiang, Z., Yu, G., Li, Y., Quinlan, E.M., Nakazawa, K., 2010. Postnatal NMDA receptor ablation in corticolimbic interneurons confers schizophrenia-like phenotypes. Nat. Neurosci. 13, 76–83.
Bhattacharya, S., Khatri, A., Swanger, S.A., DiRaddo, J.O., Yi, F., Hansen, K.B., Yuan, H., Traynelis, S.F., 2018. Triheteromeric GluN1/GluN2A/GluN2C NMDARs with unique single-channel properties are the dominant receptor population in cerebellar granule cells. Neuron 99, 315–328 e315.
Brennaman, L.H., Maness, P.F., 2010. NCAM in neuropsychiatric and neurodegenerative disorders. Adv. Exp. Med. Biol. 663, 299–317.
Brennaman, L.H., Kochlamazashvili, G., Stoenica, L., Nonneman, R.J., Moy, S.S., Schachner, M., Dityatev, A., Maness, P.F., 2011. Transgenic mice overexpressing the extracellular domain of NCAM are impaired in working memory and cortical plasticity. Neurobiol. Dis. 43, 372–378.
Brennaman, L.H., Zhang, X., Guan, H., Triplett, J.W., Brown, A., Demyanenko, G.P., Manis, P.B., Landmesser, L., Maness, P.F., 2013. Polysialylated NCAM and ephrinA/EphA regulate synaptic development of GABAergic interneurons in prefrontal cortex. In: Cerebral Cortex (New York, N.Y.: 1991), vol. 23, pp. 162–177.
Bukalo, O., Dityatev, A., 2012. Synaptic cell adhesion molecules. Adv. Exp. Med. Biol. 970, 97–128.
Bushman, J., Mishra, B., Ezra, M., Gul, S., Schulze, C., Chaudhury, S., Ripoll, D., Wallqvist, A., Kohn, J., Schachner, M., Loers, G., 2014. Tegaserod mimics the neurostimulatory glycan polysialic acid and promotes nervous system repair. Neuropharmacology 79, 456–466.
Castillo-Gomez, E., Varea, E., Blasco-Ibanez, J.M., Crespo, C., Nacher, J., 2011. Polysialic acid is required for dopamine D2 receptor-mediated plasticity involving inhibitory circuits of the rat medial prefrontal cortex. PLoS One 6, e29516.
Chen, L., Muhlhauser, M., Yang, C.R., 2003. Glycine tranporter-1 blockade potentiates NMDA-mediated responses in rat prefrontal cortical neurons in vitro and in vivo. J. Neurophysiol. 89, 691–703.
Cremer, H., Lange, R., Christoph, A., Plomann, M., Vopper, G., Roes, J., Brown, R., Baldwin, S., Kraemer, P., Scheff, S., et al., 1994. Inactivation of the N-CAM gene in mice results in size reduction of the olfactory bulb and deficits in spatial learning. Nature 367, 455–459.
Curtis, D., 2019. A possible role for sarcosine in the management of schizophrenia. Br. J. Psychiatry 215, 697–698.
Curto, Y., Alcaide, J., Röckle, I., Hildebrandt, H., 2019. Effects of the Genetic Depletion of Polysialyltransferases on the Structure and Connectivity of Interneurons in the Adult Prefrontal Cortex. Front. Neuroanat. 13, 6. https://doi.org/10.3389/fnana.2019.00006. PMID: 30787870; PMCID: PMC6372547.
Decker, J.M., Kruger, L., Sydow, A., Dennissen, F.J., Siskova, Z., Mandelkow, E., Mandelkow, E.M., 2016. The Tau/A152T mutation, a risk factor for frontotemporal-spectrum disorders, leads to NR2B receptor-mediated excitotoxicity. EMBO Rep. 17, 552–569.
Depoortere, R., Dargazanli, G., Estenne-Bouhtou, G., Coste, A., Lanneau, C., Desvignes, C., Poncelet, M., Heaulme, M., Santucci, V., Decobert, M., Cudennec, A., Voltz, C., Boulay, D., Terranova, J.P., Stemmelin, J., Roger, P., Marabout, B., Sevrin, M., Vige, X., Biton, B., Steinberg, R., Francon, D., Alonso, R., Avenet, P., Oury-Donat, F., Perrault, G., Griebel, G., George, P., Soubrie, P., Scatton, B., 2005. Neurochemical, electrophysiological and pharmacological profiles of the selective inhibitor of the glycine transporter-1 SSR504734, a potential new type of antipsychotic. In: Neuropsychopharmacology: Official Publication of the American College of Neuropsychopharmacology, 30, pp. 1963–1985.
Dityatev, A., Schachner, M., Sonderegger, P., 2010. The dual role of the extracellular matrix in synaptic plasticity and homeostasis. Nat. Rev. Neurosci. 11, 735–746.
Duncan, B.W., Murphy, K.E., Maness, P.F., 2021. Molecular mechanisms of L1 and NCAM adhesion molecules in synaptic pruning, plasticity, and stabilization. Front. Cell Dev. Biol. 9, 625340.
Eckhardt, M., Bukalo, O., Chazal, G., Wang, L., Goridis, C., Schachner, M., Gerardy-Schahn, R., Cremer, H., Dityatev, A., 2000. Mice deficient in the polysialyltransferase ST8SiaIV/PST-1 allow discrimination of the roles of neural cell adhesion molecule protein and polysialic acid in neural development and synaptic plasticity. J. Neurosci. 20, 5234–5244.
Feng, G., Mellor, R.H., Bernstein, M., Keller-Peck, C., Nguyen, Q.T., Wallace, M., Nerbonne, J.M., Lichtman, J.W., Sanes, J.R., 2000. Imaging neuronal subsets in transgenic mice expressing multiple spectral variants of GFP. Neuron 28, 41–51.
Fischer, G., Mutel, V., Trube, G., Malherbe, P., Kew, J.N., Mohacsi, E., Heitz, M.P., Kemp, J.A., 1997. Ro 25-6981, a highly potent and selective blocker of N-methyl-D-aspartate receptors containing the NR2B subunit. Characterization in vitro. J. Pharmacol. Exp. Ther. 283, 1285–1292.
France, G., Fernandez-Fernandez, D., Burnell, E.S., Irvine, M.W., Monaghan, D.T., Jane, D.E., Bortolotto, Z.A., Collingridge, G.L., Volianskis, A., 2017. Multiple roles of GluN2B-containing NMDA receptors in synaptic plasticity in juvenile hippocampus. Neuropharmacology 112, 76–83.
Gasso, P., Mas, S., Rodriguez, N., Boloc, D., Garcia-Cerro, S., Bernardo, M., Lafuente, A., Parellada, E., 2017. Microarray gene-expression study in fibroblast and lymphoblastoid cell lines from antipsychotic-naive first-episode schizophrenia patients. J. Psychiatr. Res. 95, 91–101.
Gilabert-Juan, J., Varea, E., Guirado, R., Blasco-Ibanez, J.M., Crespo, C., Nacher, J., 2012. Alterations in the expression of PSA-NCAM and synaptic proteins in the dorsolateral prefrontal cortex of psychiatric disorder patients. Neurosci. Lett. 530, 97–102.
Gomez-Climent, M.A., Guirado, R., Castillo-Gomez, E., Varea, E., Gutierrez-Mecinas, M., Gilabert-Juan, J., Garcia-Mompo, C., Vidueira, S., Sanchez-Mataredona, D., Hernandez, S., Blasco-Ibanez, J.M., Crespo, C., Rutishauser, U., Schachner, M., Nacher, J., 2011. The polysialylated form of the neural cell adhesion molecule (PSA-NCAM) is expressed in a subpopulation of mature cortical interneurons characterized by reduced structural features and connectivity. In: Cerebral Cortex (New York, N.Y.: 1991), 21, pp. 1028–1041.
Hammond, M.S., Sims, C., Parameshwaran, K., Suppiramaniam, V., Schachner, M., Dityatev, A., 2006a. Neural cell adhesion molecule-associated polysialic acid inhibits NR2B-containing N-methyl-D-aspartate receptors and prevents glutamate-induced cell death. J. Biol. Chem. 281, 34859–34869.
Hammond, M.S.L., Sims, C., Parameshwaran, K., Suppiramaniam, V., Schachner, M., Dityatev, A., 2006b. Neural cell adhesion molecule-associated polysialic acid inhibits NR2B-containing N-methyl-d-aspartate receptors and prevents glutamate-induced cell death*. J. Biol. Chem. 281, 34859–34869.
Hansen, Kasper B., Ogden, Kevin K., Yuan, H., Traynelis, Stephen F., 2014. Distinct functional and pharmacological properties of triheteromeric GluN1/GluN2A/GluN2B NMDA receptors. Neuron 81, 1084–1096.
Hardingham, G.E., Do, K.Q., 2016. Linking early-life NMDAR hypofunction and oxidative stress in schizophrenia pathogenesis. Nat. Rev. Neurosci. 17, 125–134.
Harvey, R.J., Yee, B.K., 2013. Glycine transporters as novel therapeutic targets in schizophrenia, alcohol dependence and pain. Nat. Rev. Drug. Discov. 2, 866–885. https://doi.org/10.1038/nrd3893. PMID: 24172334.
Henneberger, C., Papouin, T., Oliet, S.H., Rusakov, D.A., 2010. Long-term potentiation depends on release of D-serine from astrocytes. Nature 463, 232–236.
Hildebrandt, H., Dityatev, A., 2015. Polysialic acid in brain development and synaptic plasticity. In: SialoGlyco Chemistry and Biology I: Biosynthesis, Structural Diversity and Sialoglycopathologies. Springer Berlin Heidelberg, Berlin, Heidelberg, pp. 55–96.
Hildebrandt, H., Muhlenhoff, M., Gerardy-Schahn, R., 2010. Polysialylation of NCAM. Adv. Exp. Med. Biol. 663, 95–109.
Hinkle, C.L., Diestel, S., Lieberman, J., Maness, P.F., 2006. Metalloprotease-induced ectodomain shedding of neural cell adhesion molecule (NCAM). J. Neurobiol. 66, 1378–1395.
Honer, W.G., Falkai, P., Young, C., Wang, T., Xie, J., Bonner, J., Hu, L., Boulianne, G.L., Luo, Z., Trimble, W.S., 1997. Cingulate cortex synaptic terminal proteins and neural cell adhesion molecule in schizophrenia. Neuroscience 78, 99–110.
Huang, Y.Y., Simpson, E., Kellendonk, C., Kandel, E.R., 2004. Genetic evidence for the bidirectional modulation of synaptic plasticity in the prefrontal cortex by D1 receptors. Proc. Natl. Acad. Sci. U. S. A. 101, 3236–3241.
Iafrati, J., Orejarena, M.J., Lassalle, O., Bouamrane, L., Gonzalez-Campo, C., Chavis, P., 2014. Reelin, an extracellular matrix protein linked to early onset psychiatric diseases, drives postnatal development of the prefrontal cortex via GluN2B-NMDARs and the mTOR pathway. Mol. Psychiatry 19, 417–426.
Javitt, D.C., 2012. Glycine transport inhibitors in the treatment of schizophrenia. Handb. Exp. Pharmacol. 367–399.
Johnson, J.W., Ascher, P., 1987. Glycine potentiates the NMDA response in cultured mouse brain neurons. Nature 325, 529–531.
Kalus, I., Bormann, U., Mzoughi, M., Schachner, M., Kleene, R., 2006. Proteolytic cleavage of the neural cell adhesion molecule by ADAM17/TACE is involved in neurite outgrowth. J. Neurochem. 98, 78–88.
Keys, T.G., Freiberger, F., Ehrit, J., Krueger, J., Eggers, K., Buettner, F.F., Gerardy-Schahn, R., 2012. A universal fluorescent acceptor for high-performance liquid chromatography analysis of pro- and eukaryotic polysialyltransferases. Anal. Biochem. 427, 107–115.
Kochlamazashvili, G., Senkov, O., Grebenyuk, S., Robinson, C., Xiao, M.F., Stummeyer, K., Gerardy-Schahn, R., Engel, A.K., Feig, L., Semyanov, A., Suppiramaniam, V., Schachner, M., Dityatev, A., 2010. Neural cell adhesion molecule-associated polysialic acid regulates synaptic plasticity and learning by restraining the signaling through GluN2B-containing NMDA receptors. J. Neurosci. 30, 4171–4183.
Kochlamazashvili, G., Bukalo, O., Senkov, O., Salmen, B., Gerardy-Schahn, R., Engel, A. K., Schachner, M., Dityatev, A., 2012. Restoration of synaptic plasticity and learning in young and aged NCAM-deficient mice by enhancing neurotransmission mediated by GluN2A-containing NMDA receptors. J. Neurosci. 32, 2263–2275.
Kröcher, T., Rockle, I., Diederichs, U., Weinhold, B., Burkhardt, H., Yanagawa, Y., Gerardy-Schahn, R., Hildebrandt, H., 2014. A crucial role for polysialic acid in developmental interneuron migration and the establishment of interneuron densities in the mouse prefrontal cortex. Development (Cambridge, England) 141, 3022–3032.
Kröcher, T., Malinovskaja, K., Jurgenson, M., Aonurm-Helm, A., Zharkovskaya, T., Kalda, A., Rockle, I., Schiff, M., Weinhold, B., Gerardy-Schahn, R., Hildebrandt, H., Zharkovsky, A., 2015. Schizophrenia-like phenotype of polysialyltransferase ST8SIA2-deficient mice. Brain Struct. Funct. 220, 71–83.
Kullmann, D.M., Asztely, F., 1998. Extrasynaptic glutamate spillover in the hippocampus: evidence and implications. Trends Neurosci. 21, 8–14.
Labus, J., Röhrs, K.F., Ackmann, J., Varbanov, H., Müller, F.E., Jia, S., Jahreis, K., Vollbrecht, A.L., Butzlaff, M., Schill, Y., Guseva, D., Böhm, K., Kaushik, R., Bijata, M.,

Marin, P., Chaumont-Dubel, S., Zeug, A., Dityatev, A., Ponimaskin, E., 2021. Amelioration of Tau pathology and memory deficits by targeting 5-HT7 receptor. Prog. Neurobiol. 197, 101900.
Le Meur, K., Galante, M., Angulo, M.C., Audinat, E., 2007. Tonic activation of NMDA receptors by ambient glutamate of non-synaptic origin in the rat hippocampus. J. Physiol. 580, 373–383.
Li, S., Jin, M., Koeglsperger, T., Shepardson, N.E., Shankar, G.M., Selkoe, D.J., 2011. Soluble Aβ oligomers inhibit long-term potentiation through a mechanism involving excessive activation of extrasynaptic NR2B-containing NMDA receptors. J. Neurosci. 31, 6627–6638.
Luthi, A., Laurent, J.P., Figurov, A., Muller, D., Schachner, M., 1994. Hippocampal long-term potentiation and neural cell adhesion molecules L1 and NCAM. Nature 372, 777–779.
Muller, D., Wang, C., Skibo, G., Toni, N., Cremer, H., Calaora, V., Rougon, G., Kiss, J.Z., 1996. PSA-NCAM is required for activity-induced synaptic plasticity. Neuron 17, 413–422.
Muller-Lissner, S.A., Fumagalli, I., Bardhan, K.D., Pace, F., Pecher, E., Nault, B., Ruegg, P., 2001. Tegaserod, a 5-HT(4) receptor partial agonist, relieves symptoms in irritable bowel syndrome patients with abdominal pain, bloating and constipation. Aliment. Pharmacol. Ther. 15, 1655–1666.
Murray, H.C., Low, V.F., Swanson, M.E., Dieriks, B.V., Turner, C., Faull, R.L., Curtis, M. A., 2016. Distribution of PSA-NCAM in normal, Alzheimer's and Parkinson's disease human brain. Neuroscience 330, 359–375.
Murray, H.C., Swanson, M.E.V., Dieriks, B.V., Turner, C., Faull, R.L.M., Curtis, M.A., 2018. Neurochemical characterization of PSA-NCAM(+) cells in the human brain and phenotypic quantification in Alzheimer's disease entorhinal cortex. Neuroscience 372, 289–303.
Nacher, J., Guirado, R., Varea, E., Alonso-Llosa, G., Rockle, I., Hildebrandt, H., 2010. Divergent impact of the polysialyltransferases ST8SiaII and ST8SiaIV on polysialic acid expression in immature neurons and interneurons of the adult cerebral cortex. Neuroscience 167, 825–837.
Nacher, J., Guirado, R., Castillo-Gomez, E., 2013. Structural plasticity of interneurons in the adult brain: role of PSA-NCAM and implications for psychiatric disorders. Neurochem. Res. 38, 1122–1133.
Nelson, A.J., Cooper, M.T., Thur, K.E., Marsden, C.A., Cassaday, H.J., 2011. The effect of catecholaminergic depletion within the prelimbic and infralimbic medial prefrontal cortex on recognition memory for recency, location, and objects. Behav. Neurosci. 125, 396–403.
Paoletti, P., Bellone, C., Zhou, Q., 2013. NMDA receptor subunit diversity: impact on receptor properties, synaptic plasticity and disease. Nat. Rev. Neurosci. 14, 383–400.
Papouin, T., Oliet, S.H., 2014. Organization, control and function of extrasynaptic NMDA receptors. Philos. Trans. R. Soc. Lond. Ser. B Biol. Sci. 369, 20130601.
Papouin, T., Ladepeche, L., Ruel, J., Sacchi, S., Labasque, M., Hanini, M., Groc, L., Pollegioni, L., Mothet, J.P., Oliet, S.H., 2012. Synaptic and extrasynaptic NMDA receptors are gated by different endogenous coagonists. Cell 150, 633–646.
Sato, C., Kitajima, K., 2021. Polysialylation and disease. Mol. Asp. Med. 79, 100892.
Schnaar, R.L., Gerardy-Schahn, R., Hildebrandt, H., 2014. Sialic acids in the brain: gangliosides and polysialic acid in nervous system development, stability, disease, and regeneration. Physiol. Rev. 94, 461–518.
Seki, T., Rutishauser, U., 1998. Removal of polysialic acid-neural cell adhesion molecule induces aberrant mossy fiber innervation and ectopic synaptogenesis in the hippocampus. J. Neurosci. 18, 3757–3766.
Senkov, O., Sun, M., Weinhold, B., Gerardy-Schahn, R., Schachner, M., Dityatev, A., 2006. Polysialylated neural cell adhesion molecule is involved in induction of long-term potentiation and memory acquisition and consolidation in a fear-conditioning paradigm. J. Neurosci. 26, 10888–109898.
Senkov, O., Tikhobrazova, O., Dityatev, A., 2012. PSA-NCAM: synaptic functions mediated by its interactions with proteoglycans and glutamate receptors. Int. J. Biochem. Cell Biol. 44, 591–595.
Smith, K.E., Borden, L.A., Hartig, P.R., Branchek, T., Weinshank, R.L., 1992. Cloning and expression of a glycine transporter reveal colocalization with NMDA receptors. Neuron 8, 927–935. https://doi.org/10.1016/0896-6273(92)90207-t. PMID: 1534013.
Stoenica, L., Senkov, O., Gerardy-Schahn, R., Weinhold, B., Schachner, M., Dityatev, A., 2006. In vivo synaptic plasticity in the dentate gyrus of mice deficient in the neural cell adhesion molecule NCAM or its polysialic acid. Eur. J. Neurosci. 23, 2255–2264.
Strekalova, H., Buhmann, C., Kleene, R., Eggers, C., Saffell, J., Hemperly, J., Weiller, C., Muller-Thomsen, T., Schachner, M., 2006. Elevated levels of neural recognition molecule L1 in the cerebrospinal fluid of patients with Alzheimer disease and other dementia syndromes. Neurobiol. Aging 27, 1–9.
Stummeyer, K., Dickmanns, A., Muhlenhoff, M., Gerardy-Schahn, R., Ficner, R., 2005. Crystal structure of the polysialic acid-degrading endosialidase of bacteriophage K1F. Nat. Struct. Mol. Biol. 12, 90–96.
Tackenberg, C., Brandt, R., 2009. Divergent pathways mediate spine alterations and cell death induced by amyloid-beta, wild-type tau, and R406W tau. J. Neurosci. 29, 14439–14450.
Thiesler, H., Kucukerden, M., Gretenkort, L., Rockle, I., Hildebrandt, H., 2022. News and views on polysialic acid: from tumor progression and brain development to psychiatric disorders, neurodegeneration, myelin repair and immunomodulation. Front. Cell Dev. Biol. 10, 871757.
Todaro, L., Puricelli, L., Gioseffi, H., Guadalupe Pallotta, M., Lastiri, J., Bal de Kier Joffe, E., Varela, M., Sacerdote de Lustig, E., 2004. Neural cell adhesion molecule in human serum. Increased levels in dementia of the Alzheimer type. Neurobiol. Dis. 15, 387–393.
Varbanov, H., Dityatev, A., 2017. Regulation of extrasynaptic signaling by polysialylated NCAM: impact for synaptic plasticity and cognitive functions. Mol. Cell. Neurosci. 81, 12–21.
Vawter, M.P., 2000. Dysregulation of the neural cell adhesion molecule and neuropsychiatric disorders. Eur. J. Pharmacol. 405, 385–395.
Vawter, M.P., Cannon-Spoor, H.E., Hemperly, J.J., Hyde, T.M., VanderPutten, D.M., Kleinman, J.E., Freed, W.J., 1998. Abnormal expression of cell recognition molecules in schizophrenia. Exp. Neurol. 149, 424–432.
Volianskis, A., Bannister, N., Collett, V.J., Irvine, M.W., Monaghan, D.T., Fitzjohn, S.M., Jensen, M.S., Jane, D.E., Collingridge, G.L., 2013. Different NMDA receptor subtypes mediate induction of long-term potentiation and two forms of short-term potentiation at CA1 synapses in rat hippocampus in vitro. J. Physiol. 591, 955–972.
Williams, S.E., Mealer, R.G., Scolnick, E.M., Smoller, J.W., Cummings, R.D., 2020. Aberrant glycosylation in schizophrenia: a review of 25 years of post-mortem brain studies. Mol. Psychiatry 25, 3198–3207.
Yi, F., Bhattacharya, S., Thompson, C.M., Traynelis, S.F., Hansen, K.B., 2019. Functional and pharmacological properties of triheteromeric GluN1/2B/2D NMDA receptors. J. Physiol. 597, 5495–5514.
Zott, B., Simon, M.M., Hong, W., Unger, F., Chen-Engerer, H.-J., Frosch, M.P., Sakmann, B., Walsh, D.M., Konnerth, A., 2019. A vicious cycle of β amyloid-dependent neuronal hyperactivation. Science 365, 559–565.